USGS
science for a changing world

Geohydrology and Numerical Simulation of Alternative Pumping Distributions and the Effects of Drought on the Ground-Water Flow System of Tinian, Commonwealth of the Northern Mariana Islands

U.S. Department of the Interior
U.S. Geological Survey
Water-Resources Investigations Report 02-4077

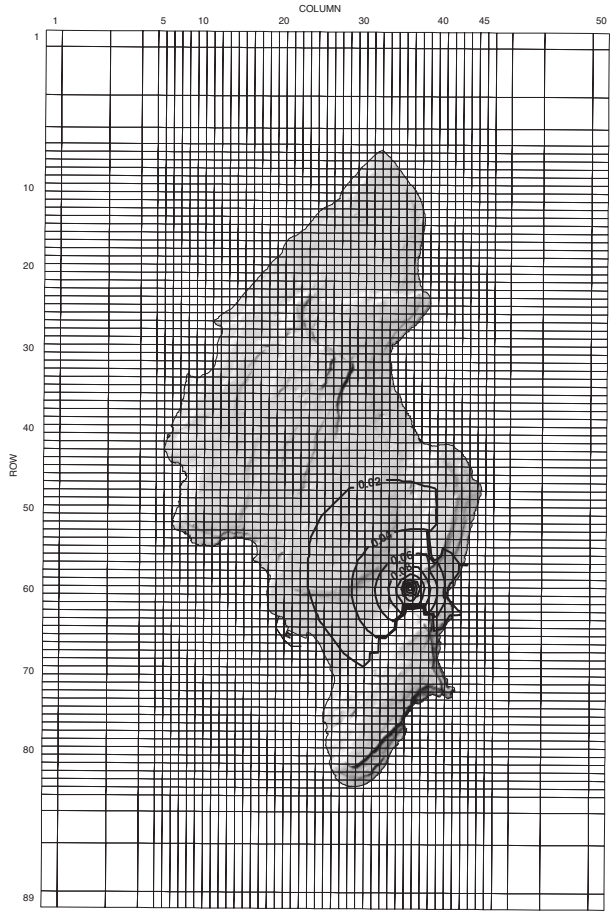

Prepared in cooperation with the
COMMONWEALTH UTILITIES CORPORATION, COMMONWEALTH OF THE NORTHERN MARIANA ISLANDS

Geohydrology and Numerical Simulation of Alternative Pumping Distributions and the Effects of Drought on the Ground-Water Flow System of Tinian, Commonwealth of the Northern Mariana Islands

---

By Stephen B. Gingerich

U.S. GEOLOGICAL SURVEY
Water-Resources Investigations Report 02-4077

Prepared in cooperation with the

COMMONWEALTH UTILITIES CORPORATION, COMMONWEALTH OF THE NORTHERN MARIANA ISLANDS

Honolulu, Hawaii
2002

U.S. DEPARTMENT OF THE INTERIOR

GALE A. NORTON, Secretary

U.S. GEOLOGICAL SURVEY

Charles G. Groat, Director

The use of firm, trade, and brand names in this report is for identification purposes only and does not constitute endorsement by the U.S. Geological Survey.

For additional information write to:

District Chief
U.S. Geological Survey
677 Ala Moana Blvd., Suite 415
Honolulu, HI 96813

Copies of this report can be purchased from:

U.S. Geological Survey
Branch of Information Services
Box 25286
Denver, CO 80225-0286

CONTENTS

FIGURES

TABLES

Geohydrology and Numerical Simulation of Alternative Pumping Distributions and the Effects of Drought on the Ground-Water Flow System of Tinian, Commonwealth of the Northern Mariana Islands

By Stephen B. Gingerich

Abstract

Ground water in a freshwater lens is the main source of freshwater on Tinian, Commonwealth of the Northern Mariana Islands. Four major geologic units make up the island with high-permeability limestone units overlying low-permeability volcanic rocks. Estimates of limestone hydraulic conductivity range from 21 to 23,000 feet per day.

Estimates of water-budget components for Tinian are 82 inches per year of rainfall, about 6 inches per year of runoff, 46 inches per year of evapotranspiration, and 30 inches per year of recharge. From 1990–97, ground-water withdrawal from the Municipal well, the major source of water, averaged about 780 gallons per minute.

A two-dimensional, steady-state, ground-water flow model using the computer code SHARP was developed for Tinian, to enhance the understanding of (1) the distribution of aquifer hydraulic properties, (2) the conceptual framework of the ground-water flow system, and (3) the effects of various pumping distributions and drought on water levels and the freshwater/saltwater transition zone. For modeling purposes, Tinian was divided into three horizontal hydraulic-conductivity zones: (1) highly permeable limestone, (2) less-permeable, clay-rich limestone, and (3) low-permeability volcanic rocks.

The following horizontal hydraulic conductivities were estimated: (1) 10,500 feet per day for the highly permeable limestone, (2) 800 feet per day for the less-permeable clay-rich limestone, and (3) 0.2 foot per day for the volcanic rocks.

To estimate the hydrologic effects of different pumping distributions on the aquifer, three different steady-state pumping scenarios were simulated, (1) a scenario with no ground-water pumping, (2) a 2001-pumping scenario, and (3) a maximum-pumping scenario.

The results of the no-pumping scenario showed that the freshwater/saltwater interface beneath the Municipal well would be about 7 feet deeper and ground-water discharge to the coast would be higher along both the east and west coasts of the island when compared with 1990–97 pumping conditions. For the maximum pumping scenario, the model-calculated freshwater/saltwater interface is about 7 feet shallower than the position calculated in the base-case scenario.

To estimate the hydrologic effects of drought on the freshwater lens, the 2001- and maximum-pumping scenarios were simulated using three combinations of aquifer porosity values covering a range of possible limestone properties. In all scenarios, recharge was reduced to 10 percent of average estimated recharge and the transient response was simulated for 1 year. These simulations demonstrated that the ground-water resource is adequate to withstand a drought similar to that experienced in 1998 using existing infrastructure.

INTRODUCTION

On the island of Tinian, Commonwealth of the Northern Mariana Islands (CNMI), fresh ground water is obtained from shallow wells that tap the surface of a relatively thin freshwater lens found in an aquifer composed mainly of coralline limestone. During 1998, a severe drought affected the western Pacific and as a result, Tinian received less than half of its average annual rainfall. The water supply on Tinian provided water without disruption throughout the drought, but as demands increase in the future, it becomes increasingly likely that supplies could be affected by drought, mainly by the increase of salinity of the pumped water. Because of the drought, the Federal Emergency Management Agency (FEMA) provided assistance and funds to help mitigate the problem. To better understand the ground-water resources of the island and the potential effects of drought on the island's water supply, the U.S. Geological Survey (USGS) entered into a cooperative study with the Commonwealth Utilities Corporation (CUC) of the CNMI with funding provided by FEMA. The study objective is to provide information to help water managers be prepared for the next drought and its effects on the island's water supply.

Purpose and Scope

The purpose of this report is to describe (1) the geologic and hydrologic setting of Tinian, (2) the numerical ground-water flow model developed, (3) the results of the model simulations that assess the hydrologic effects of drought on the freshwater lens, and (4) data needs. No new data were collected for this report; only existing data were used to develop the conceptual framework of the ground-water flow system. A numerical ground-water flow model of Tinian was used to refine the conceptual framework and to estimate the effects of different withdrawal scenarios and drought on ground-water levels, the freshwater/saltwater interface, and coastal discharge.

Description of Study Site

Physical Setting

Tinian, which lies in the western Pacific Ocean at latitude 15°N and longitude 145°E (fig. 1), is the second largest island (39.2 mi^2) in the CNMI. The island of Tinian is about 12 mi long and as much as 6 mi wide. The surface landforms can be divided into five major physiographic areas (Doan and others, 1960) (fig. 1).

The southeastern ridge is the southernmost and highest part of the island and consists of northern and southern ridges, separated by a gap near the midpoint. Steep slopes and cliffs that are as much as 500 ft high form the southeast boundary of the ridge. The highest point on Tinian is Mt. Kastiyu on the southern ridge, at 614 ft altitude. To the northwest, the median or Marpo Valley, a low, broad depression that separates the southeastern ridge from the central plateau, reaches an altitude of about 150 ft. The land surface intersects the water table at a depression in the valley, forming the Marpo Marsh, a wetland with a small area of shallow surface water. The central plateau extends northward and constitutes all of central and some of the northern part of Tinian. The central plateau is broad and gently sloping with principal relief along its boundaries with the median valley and northern lowland. The north-central highland rises within the northern part of the central plateau, midway between the eastern and western coasts. The highest point of the north-central highland, 545 ft altitude, is exceeded in height only on the southeastern ridge. The northern lowland generally is flat and about 100 ft in altitude except at Hagoi Lake where the altitude is near sea level. Hagoi Lake is a fresh to brackish water body surrounded by a marsh. The area of surface water may extend to one-half mile in length during the wet season, and decrease to a marsh with little surface water during the dry season.

Land Use

The population of Tinian, 2,631 people in 1995 (Bureau of Census, 1996), resides around rural San Jose Village located in the median valley and parts of the adjacent central plateau and southeastern ridge (Baldwin, 1995) (fig. 2). Most public and residential land-use activities take place in this area. Public land includes the airport, harbor, schools, cemetery, agricultural cooperatives, Marpo Marsh, parks and beaches, and some unused grassland and secondary forest. Residential and commercial land includes a casino resort, small businesses, farming, grazing, and housing.

About 75 percent of the island is grassland and secondary forest supporting minor land-use activities. About 30 percent of the grassland is reserved exclusively for military use in the northern part of the island, except for a U.S. Information Agency radio station

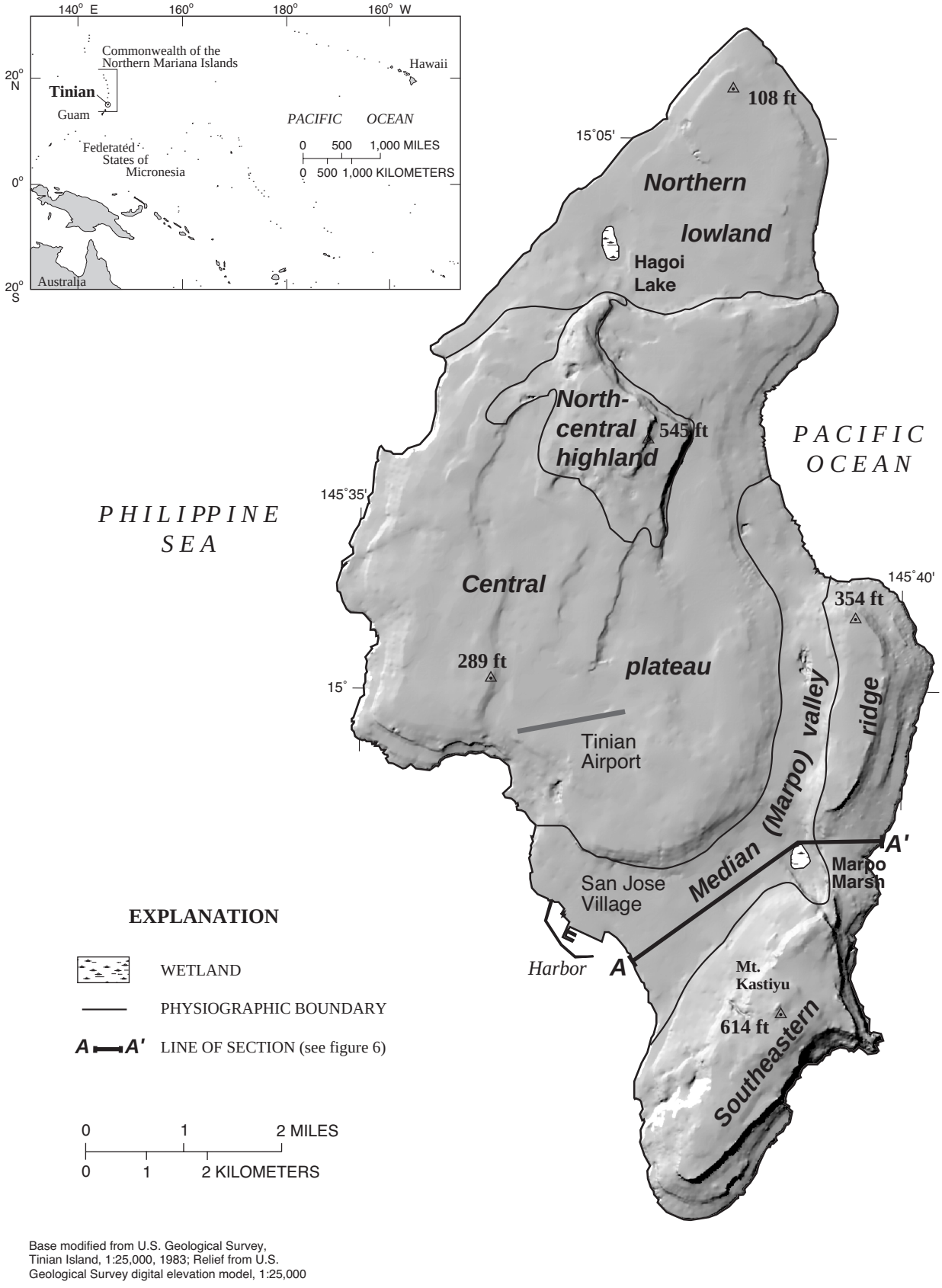

Base modified from U.S. Geological Survey, Tinian Island, 1:25,000, 1983; Relief from U.S. Geological Survey digital elevation model, 1:25,000

Figure 1. Location map and physiographic areas of Tinian (modified from Doan and others, 1960).

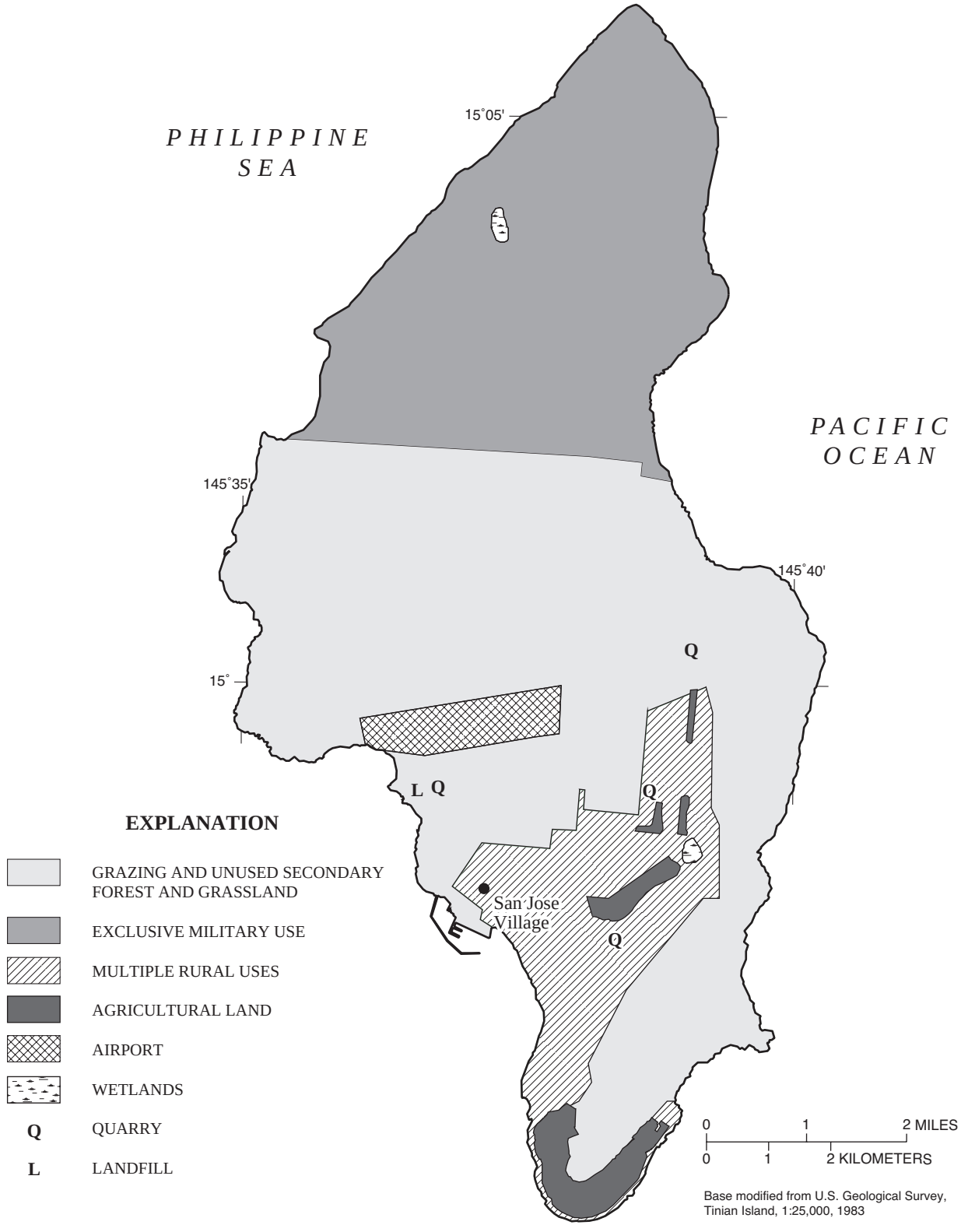

Figure 2. Generalized land use, Tinian (modified from U.S. Geological Survey, 1983; Young, 1989; and U.S. Department of Agriculture, 1994).

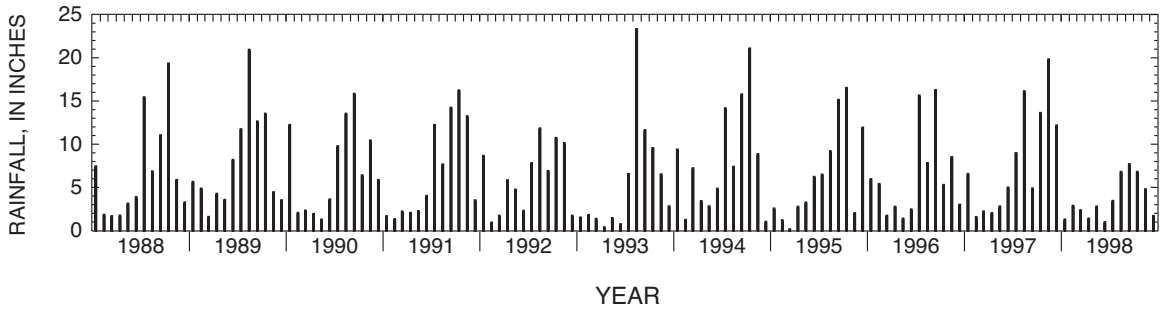

Figure 3. Monthly rainfall at airport, 1988–98, Tinian (National Climatic Data Center, 2000).

operating in the southwestern part of this area. About 45 percent of the remaining grassland and secondary forest, mostly on the central plateau and southeastern ridge, is used for scattered grazing of cattle and horses.

Climate

Seasonal differences in rainfall define distinct wet and dry seasons on Tinian (fig. 3). The months of July through October (the wet season) receive about 61 percent (49 in.) of the annual rainfall; February through May (the dry season) receive 12 percent (10 in.) of the rainfall; and November, December, January, and June (transitional months) receive 27 percent (22 in.) of the rainfall. From 1988 to 1998, the total annual rainfall ranged from a low of 43 in. in 1998 to a high of 97 in. in 1994. The lowest amount of monthly rainfall recorded for the period of record was 0.13 in. during March 1995. The highest daily rainfall amount recorded for the period of record was 12.9 in. on August 6, 1993 during tropical storm Steve. Rainfall from tropical storms and typhoons make up a significant percentage of the total annual rainfall and a lack of storms can significantly contribute to drought conditions.

HYDROGEOLOGY

Four major geologic units make up the island (fig. 4). They are the Tinian Pyroclastic Rocks, the Tagpochau Limestone, the Mariana Limestone, and unconsolidated sediments consisting of beach deposits, alluvium, and colluvium. Hydraulic conductivity of the island's aquifers depends on the rock type constituting the aquifers.

Geology

The Tinian Pyroclastic Rocks, of late Eocene age, is the oldest exposed geologic unit and probably underlies all other exposed rock units (Doan and others, 1960). This unit is exposed in the north-central highland and southeastern ridge and covers about 2 percent of the surface of the island. The thickness of the unit is unknown because the position of the base is undetermined. The Tinian Pyroclastic Rocks consists of fine to coarse-grained consolidated ash and angular fragments of volcanic origin. Outcrops usually are highly weathered and altered to clay.

The Tagpochau Limestone is of early Miocene age (Doan and others, 1960) and is exposed on about 15 percent of the surface on Tinian, principally in the north-central highland and the southern part of the southeastern ridge. The unit thickens from 0 to at least 600 ft thick in all directions away from the surface exposures of the Tinian Pyroclastic Rocks in the north-central highland and southeastern ridge. The Tagpochau Limestone is composed of fine to coarse-grained, partially recrystallized broken limestone fragments, and about 5 percent reworked volcanic fragments and clays. Surface exposures are highly weathered.

The Mariana Limestone is of Pliocene to Pleistocene age and is the most extensive unit areally and volumetrically above sea level covering about 80 percent of the surface, and forming nearly all of the northern lowlands, the central plateau, and the median valley. The Mariana Limestone thickens from 0 to at least 450 ft thick in all directions away from the surface exposures of the Tinian Pyroclastic Rocks and the

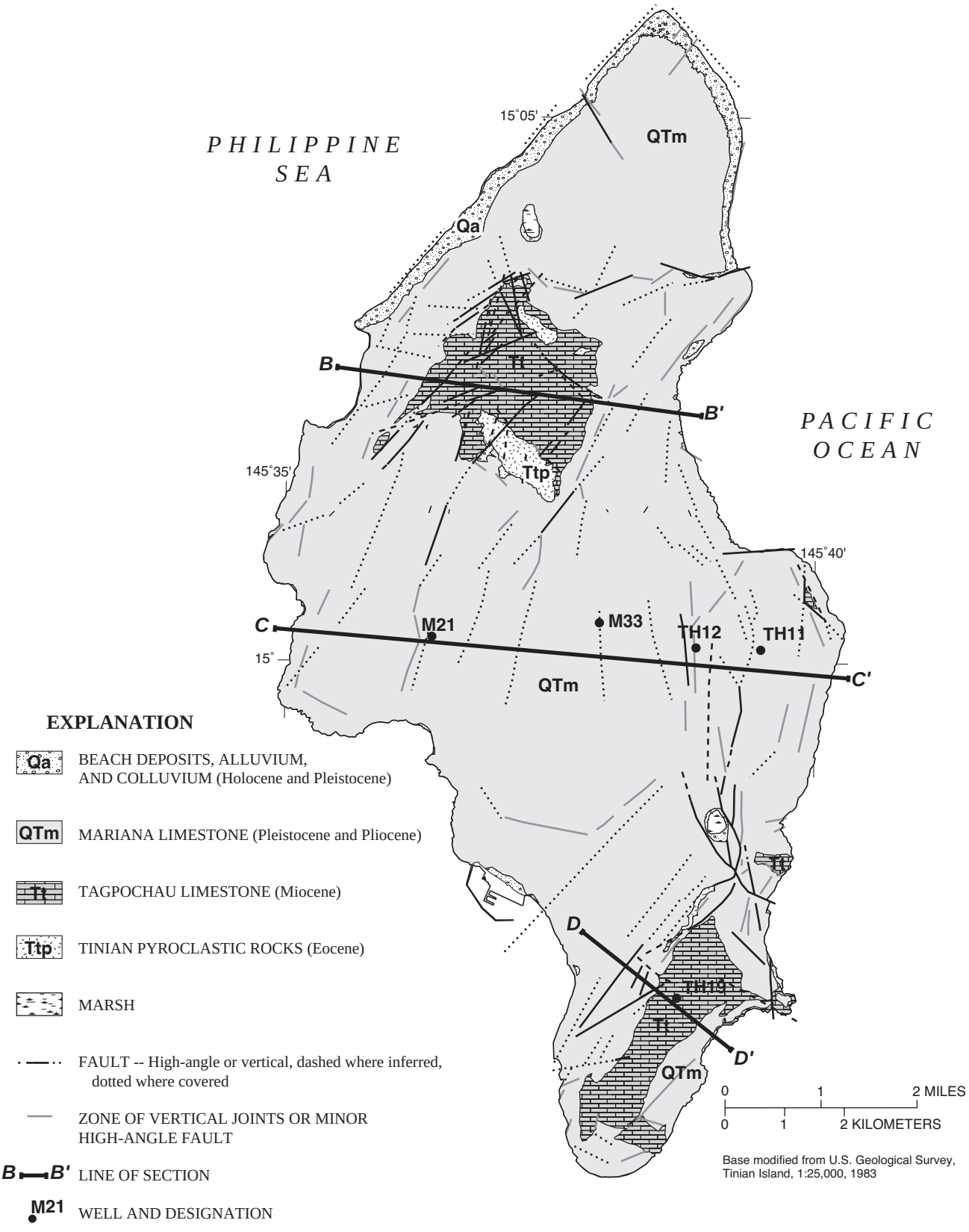

Figure 4. Generalized surficial geology and geologic sections, Tinian (modified from Doan and others, 1960).

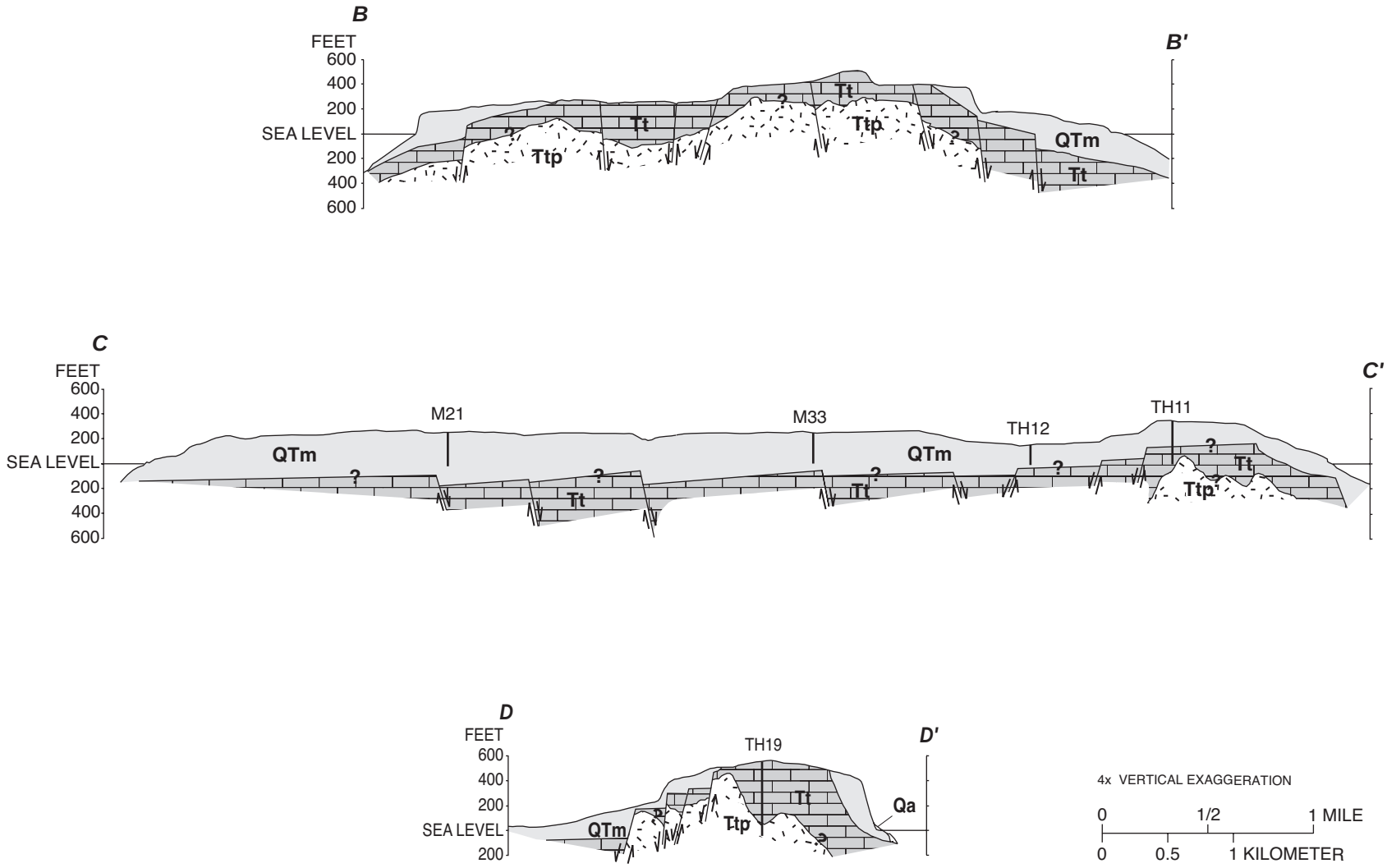

Figure 4. Generalized surficial geology and geologic sections, Tinian (modified from Doan and others, 1960)--Continued.

Table 1. Summary of aquifer-test data, Tinian, CNMI

[ft, feet; ft^3/day, cubic feet per day; ft/day, feet per day; QTm, Mariana Limestone; Tt, Tagpochau Limestone; Ttp, Tinian Pyroclastic Rocks; well loss was not subtracted from steady-state drawdown; well locations shown on fig. 7]

Pumped-well name	Starting date of test	Duration of test (days)	Radius of well, r_w (ft)	Pumping rate, Q (ft^3/day)	Steady-state drawdown, S_s (ft)	Open or screened interval of pumped well, L (ft)	Hydraulic conductivity, K (ft/day)	Geologic unit
M07	6/1/95	3	0.25	4,428	6.73	20	25	QTm, Tt
M09	4/25/95	3	0.25	24,642	0.17	16	6,700	QTm, Tt
M11	4/19/95	3	0.25	23,872	1.95	15	590	QTm, Tt
M16	5/25/95	2	0.33	18,481	1.07	18	680	QTm, Tt
M19	11/1/00	2	0.25	5,775	7.01	16	38	Tt
M21	10/31/00	3	0.25	9,433	0.19	18	2,100	QTm, Tt
TH01	10/28/96	1	0.50	31,765	0.18	12	8,500	QTm, Tt
TH03	6/9/97	2	0.33	20,214	0.14	23	4,700	QTm, Tt
TH04	5/3/94	2	0.33	20,791	0.60	19	1,300	QTm, Tt
TH05	2/14/96	2	0.33	17,711	0.55	19	1,200	QTm, Tt
TH06	3/8/95	3	0.66	10,973	0.02	13	23,000	QTm, Tt
TH07	2/1/95	2	0.66	9,626	13.5	21	21	QTm, Tt
TH10	11/4/00	5	0.33	13,091	0.19	17	2,800	QTm, Tt
TH11	9/4/97	2	0.25	12,128	4.17	18	122	QTm, Tt
TH12	11/6/00	5	0.33	13,861	0.09	14	7,400	QTm, Tt
TH22	6/2/97	3	0.33	21,176	0.11	17	8,000	Ttp
TH24	6/30/97	1	0.33	578[a]	6[a]	10	6[a]	

[a] values are estimates because well went dry after 4 minutes of pumping

Tagpochau Limestone. The Mariana Limestone is composed of fine to coarse-grained fragmented limestone, commonly coralliferous, with some fossil and algal remains, and lesser amounts of clay particles (Doan and others, 1960). Small voids and caverns are common in surface exposures. The Mariana Limestone differs from the Tagpochau Limestone in its higher coral content and lesser degree of recrystallization.

The beach deposits, alluvium, and colluvium are of Pleistocene to Holocene age. These deposits cover less than 1 percent of the surface of Tinian, and may be as much as 15 ft thick. The deposits are composed of poorly consolidated sediments, mostly calcareous sand and gravel deposited by waves, but also clays and silt deposited inland beside Hagoi Lake and Marpo Marsh, and loose soil and rock material deposited at the base of slopes, especially in the north-central highlands.

Hydraulic Conductivity

Hydraulic conductivity is a quantitative measure of the capacity of a rock to transmit water. The porous and well-washed character of coral reefs, and the high susceptibility of limestone to solution weathering favor high hydraulic conductivities in the limestone units. In contrast, hydraulic conductivities of the pyroclastic rocks tend to be low due to poor sorting and the high susceptibility of some volcanic minerals to chemical weathering and alteration to clays.

Estimates of hydraulic conductivity were made from single-well aquifer tests done on Tinian by the USGS (table 1). The method presented by Harr (1962) and Polubarinova-Kochina (1962) can be used to obtain estimates of the conductivity of a thick, unconfined aquifer that is penetrated only partially by a pumped well assuming drawdown in the well is at a “steady-state” condition. Drawdown in a pumping well and the surrounding aquifer system will proceed until the well discharge is balanced by recharge captured by the cone of depression in the aquifer system, at which time the system is in equilibrium or at “steady-state”. As the system approaches steady state, measurable incremental drawdown in the pumping well commonly becomes impractical to measure after a period of sustained

pumping, especially in an aquifer of high hydraulic conductivity. The amount of maximum drawdown in this situation can be considered "steady-state" for this analysis. Well-construction and aquifer-test information are used in the following equation to estimate aquifer hydraulic conductivity:

$$K = \frac{Q}{2\pi L s_s} ln\left(1.6\frac{L}{r_w}\right) \quad (1)$$

where:

K = hydraulic conductivity [L/T]
Q = withdrawal rate [L^3/T],
π = the number pi, 3.1415927,
L = length of open interval of pumped well [L],
s_s = steady-state drawdown in pumped well [L], and
r_w = radius of pumped well [L].

Pumping rates for the tests ranged from 3 gal/min (578 ft^3/day) to 165 gal/min (31,765 ft^3/day) and test lengths ranged from 1 to 5 days. The estimates of hydraulic conductivity in limestone on Tinian ranged from 21 to 23,000 ft/d. The lowest values are interpreted to be from limestone having a higher percentage of alluvial clay weathered from nearby volcanic rock. One estimate of hydraulic conductivity from the Tinian Pyroclastic Rocks was 6 ft/d for a well that went dry 4 minutes after the beginning of the test. This estimate is an upper bound on the hydraulic conductivity of the Tinian Pyroclastic Rocks because the well was not able to reach a steady-state condition before becoming dry. Estimates of hydraulic conductivity from the Mariana Limestone forming the Kagman Peninsula on Saipan range from 290 to 2,500 ft/d (Hoffmann and others, 1998).

Faults

Normal faults transect the island throughout, displacing rock units relative to one another, generally by less than 100 ft. The regional strike of the faults is north-south, approximately parallel to the trend axis of the Mariana Arc. Faults in limestone exposed at the surface commonly show weathered gaps along the fault, ranging from a few inches to several feet in width; thus, faults in limestone may represent narrow zones of relatively higher permeability than surrounding rock. The Tinian Pyroclastic Rocks and Tagpochau Limestone are dissected by faults concealed by the Mariana Limestone.

WATER BUDGET

Fresh ground water on Tinian is derived from precipitation, mainly rain. The rain either (1) runs off, (2) evaporates or is transpired by vegetation, or (3) recharges the ground-water system. Recharge for Tinian was estimated for this study using a variant of a water-budget accounting procedure (Thornthwaite and Mather, 1955). Daily runoff (R_i) was subtracted from daily rainfall (P_i), and this volume was added to the beginning soil-moisture storage for the current day (S_{i-1}) to determine an interim soil-moisture storage (X_i):

$$X_i = P_i - R_i + S_{i-1} \quad (2)$$

where:

X_i = interim soil-moisture storage for current day [L],
P_i = rainfall for current day [L],
R_i = runoff for current day [L],
S_{i-1} = ending soil-moisture storage from previous day (i-1), equal to the beginning available soil-moisture storage for current day (i) [L], and
i = subscript designating current day number.

All water volumes are expressed as an equivalent depth of water over an area by dividing by the total area. Soil-moisture storage, expressed as a water depth, is the product of the plant root depth (D) and the difference between the beginning volumetric soil-moisture content within the root zone for the current day (θ_{i-1}) and the volumetric wilting-point moisture content (θ_{wp}):

$$S_{i-1} = D \times (\theta_{i-1} - \theta_{wp}) \quad (3)$$

where:

D = plant root depth [L],
θ_{i-1} = ending volumetric soil-moisture content from previous day (i-1), equal to the beginning volumetric soil-moisture content within the root zone for current day (i) [L^3/L^3], and
θ_{wp} = volumetric wilting-point moisture content [L^3/L^3].

The maximum soil-moisture storage capacity (S_m) is the product of the plant root depth (D) and the available water capacity (ϕ), which is the difference between

the volumetric field-capacity moisture content (θ_{fc}) and the volumetric wilting-point moisture content (θ_{wp}).

$$S_m = D \times \phi \quad (4)$$

$$\phi = \theta_{fc} - \theta_{wp}$$

where:

S_m = maximum soil-moisture storage capacity [L],
ϕ = available water capacity [L^3/L^3], and
θ_{fc} = volumetric field-capacity moisture content [L^3/L^3].

In the accounting procedure, evapotranspiration (E_i) is subtracted from the interim soil-moisture storage (X_i), and any soil moisture (S_i) remaining greater than the soil-moisture storage capacity (S_m) is assumed to be ground-water recharge (Q_i). Evapotranspiration was determined as a function of soil moisture and potential evapotranspiration using the average of two models, Veihmeyer and Hendrickson (1955) and Thornthwaite and Mather (1955). Veihmeyer and Hendrickson (1955) suggested that evapotranspiration (E_i) occurs at the potential evapotranspiration rate (PE_i) as soil moisture is reduced from field capacity to the wilting point, but that the evapotranspiration rate decreases sharply (step-wise model) as soil moisture approaches the wilting point:

$$E_i = PE_i \text{ for } X_i \geq PE_i \quad (5)$$

$$E_i = X_i \text{ for } X_i < PE_i$$

where:

E_i = depth of water lost to evapotranspiration during the current day [L], and
PE_i = potential evapotranspiration for current day [L].

Thornthwaite and Mather (1955) suggested that the evapotranspiration rate decreases linearly as soil moisture is reduced from field capacity to the wilting point which leads to:

$$E_i = PE_i t_i + S_m\{1 - \exp[-PE_i(1 - t_i)/S_m]\}$$

$$\text{for } X_i > S_m,\ t_i < 1; \quad (6)$$

$$E_i = PE_i \text{ for } X_i > S_m,\ t_i \geq 1;$$

$$E_i = X_i\{1 - \exp[-PE_i/S_m]\} \text{ for } X_i \leq S_m;$$

$$t_i = (X_i - S_m)/PE_i$$

where:

t_i = time during which soil-moisture storage is above S_m [T].

Ground-water recharge (Q_i) and soil-moisture storage at the end of current day (S_i) are determined as:

$$Q_i = X_i - E_i - S_m; \quad (7)$$

$$S_i = S_m \text{ for } X_i - E_i > S_m;$$

$$Q_i = 0;$$

$$S_i = X_i - E_i \text{ for } X_i - E_i \leq S_m$$

where:

Q_i = ground-water recharge on current day [L], and
S_i = soil-moisture storage at the end of current day [L].

Precipitation

Precipitation, mainly in the form of rainfall, has averaged about 81 in/yr at the airport weather station during 1988 to 1994 and 1996 when complete records of daily rainfall are available (National Climatic Data Center, 2000). Because the highest point on Tinian is only 624 ft above sea level, orographic effects on rainfall appear to be small. The U.S. Geological Survey measured rainfall at four sites on Tinian during 1993 to 1996 and the measured amounts ranged from 72 to 82 in/yr across the island. Most of the difference between gages can be attributed to localized storms, and would be expected to average out given a longer period of record. For the water-budget calculation, daily rainfall values at the airport during October 13, 1987 to August 31, 1997 were used. Where daily rainfall values were missing (7 percent of the data), estimates were made using daily data from nearby USGS raingages. Average annual rainfall for the water budget using this data is about 82 in/yr.

Runoff

No perennial streams flow on Tinian and there are no records of streamflow or runoff. Runoff is expected after intense rainfall (Baldwin, 1995) but amounts have not been quantified. Rough estimates of runoff from the limestone areas of Saipan range from 6 to 12 percent of

Table 2. Monthly and annual pan-evaporation data, Guam

[all values are in inches; 1956 to May 1958 at Fena Reservoir, Aug. 1958 to Dec. 1982 at Weather Service Station; Source: National Climatic Data Center]

Jan.	Feb.	Mar	Apr.	May	June	July	Aug.	Sep.	Oct.	Nov.	Dec.	Ann.
5.98	6.14	7.54	7.99	8.03	7.02	6.11	5.56	5.22	5.45	5.65	5.96	76.65

rainfall (Cox and Evans, 1956; Belt, Collins & Associates, 1983). For the water-budget calculation, runoff was assumed to average 7.5 percent of rainfall regardless of the intensity or amount of rain recorded.

Evapotranspiration

Evapotranspiration is the quantity of water evaporated from soil and water surfaces and from plant transpiration, which is the vaporization of water through the plant's stomata (Brutsaert, 1982). Evapotranspiration estimates can best be made using several methods including the use of field measurements made using evaporimeters or lysimeters, or by using various climatic data and crop information. For Tinian, these data are not available, so evapotranspiration was estimated using pan-evaporation data from Guam and Tinian soil data.

Pan Evaporation and Potential Evapotranspiration

In water-budget studies on tropical islands where evapotranspiration data are lacking, potential evapotranspiration is commonly assumed equal to evaporation on the basis of experiments done on Hawaii (Ekern, 1966). No records of evaporation have been published for Tinian. The nearest sites where pan-evaporation data were collected are on Guam, about 100 mi south of Tinian (table 2). Because these data are monthly values, for the water-budget calculation, each value was divided by the number of days in the month to determine an average daily value of pan evaporation (hence, potential evapotranspiration assuming the two values are equal). The use of Guam potential evaporation data for Tinian is not ideal but is reasonable assuming that evaporation on the two islands is similar. Nullet (1987), in a study of potential evapotranspiration (PE) on atoll islands, estimated that PE near Tinian and Guam decreases to the north at a rate of about 4 in/yr per 10 degrees of latitude. This equates to a decrease from Guam to Tinian of about 0.6 in/yr. This difference is considered small so the Guam evaporation data were used without modification.

Soil Characteristics

Soils of Tinian have been mapped (fig. 5) and their characteristics tabulated by the Soil Conservation Service (Young, 1989). The root depth was assumed to be the average of the values reported for the effective rooting depth (table 3). For soils that the rooting depth was reported as "greater than" some depth, the actual value used was 1.5 times that reported depth. The available water capacity used was the average of the range reported (table 11 in Young, 1989). The area-weighted average available soil-moisture storage capacity was estimated to be 2.3 in. (19.25 in. × 0.121 in/in). A reasonable range of soil-moisture storage capacity values is 0.4 to 3.0 in. For a minimum estimate all soil is assumed to be rock outcrop with a minimum root depth and available water capacity (5 in. × 0.08 in/in) and for a maximum estimate, all soil is assumed to be Chinen clay loam with a maximum root depth and available water capacity (20 in. × 0.15 in/in).

Water-Budget Results

The average annual recharge for the entire island was estimated to be about 30 in/yr using the bookkeeping method on daily rainfall data during 1987 to 1997. The linear evapotranspiration model of Thornthwaite and Mather (1955) provided a recharge estimate of 32 in/yr and the step model of Veihmeyer and Hendrickson (1955) provided an estimate of 27 in/yr. The averaged estimate of annual evapotranspiration was about 46 in/yr (43 in/yr for the linear method and 48 in/yr for the step method). Runoff was estimated to be about 6 in/yr.

A reasonable range of recharge estimates can be made by calculating the daily water budget using estimates of the extremes of runoff (6 and 12 percent) and soil-moisture storage capacity (0.4 and 3.0 in.). Maximum recharge, when runoff and soil-moisture storage capacity are at a minimum, was calculated to be 41 in/yr

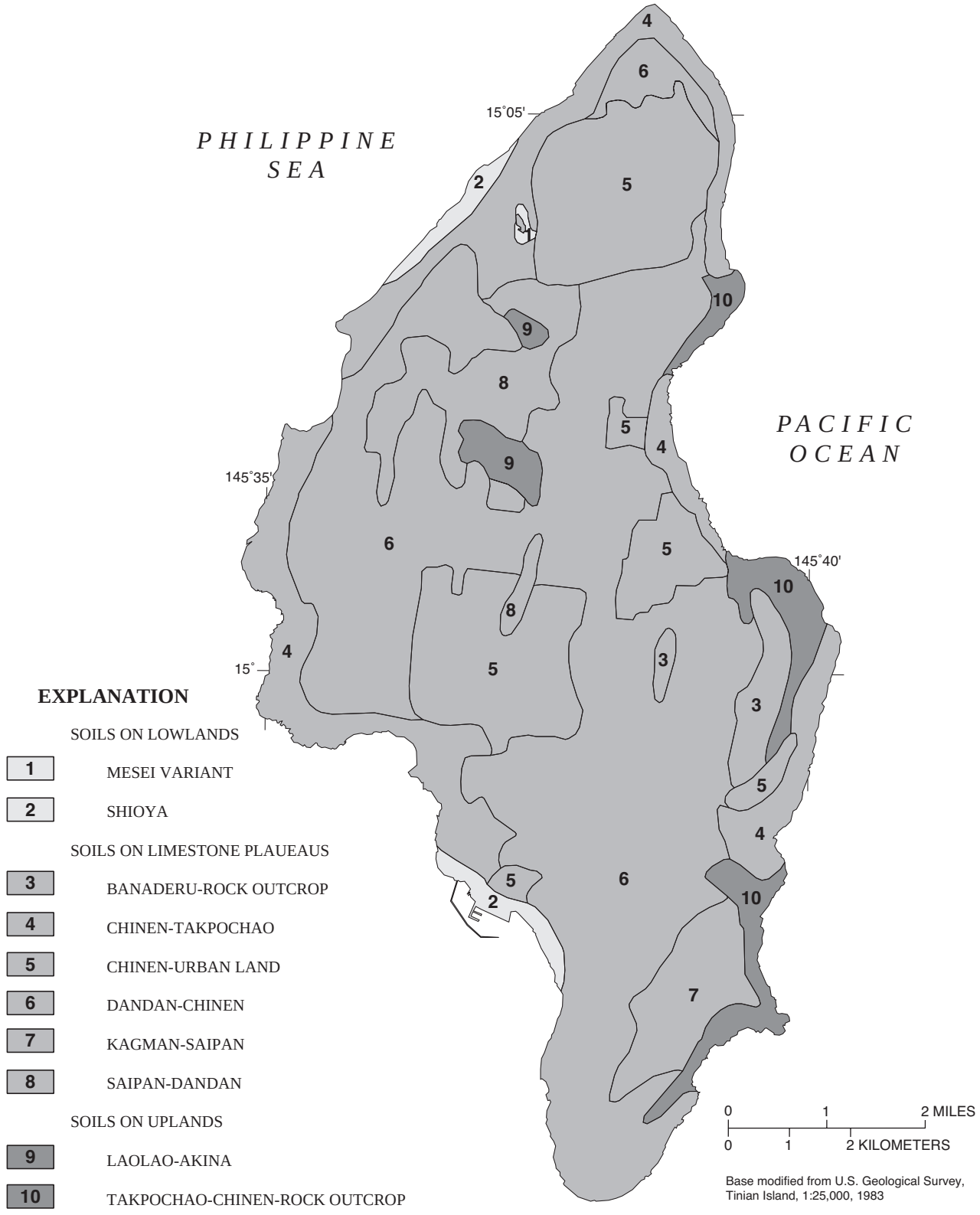

Figure 5. Generalized soil distribution, Tinian (modified from Young, 1989).

Table 3. Average soil characteristics, Tinian

[in, inches; in/in, inch per inch of soil; average root depth is the average of the range of rooting depths and available water capacity is the average of the range described in Young, 1989]

Soil name	Area (relative to entire island)	Average root depth (in)	Area-weighted average root depth (in)	Available water capacity (in/in)	Area-weighted available water capacity (in/in)
Banaderu clay loam	0.020	14.8	0.30	0.137	0.003
Chacha clay	0.001	88.6	0.09	0.125	1.25×10^{-4}
Chinen clay loam; Chinen rock outcrop complex; Chinen-Urban land complex; Dandan-Chinen complex; Dandan-Chinen-Pits complex, 5 to 15 percent slopes	0.687	14.8	10.17	0.125	0.086
Chinen very gravelly sandy loam, 0 to 5 percent slopes	0.009	14.8	0.13	0.093	0.001
Chinen very gravelly sandy loam, 5 to 15 percent slopes	0.043	25.6	1.10	0.097	0.004
Dandan-Chinen-Pits complex, 0 to 5 percent slopes	0.015	29.5	0.44	0.125	0.002
Dandan-Saipan clays, 0 to 5 percent slopes	0.029	29.5	0.86	0.120	0.003
Dandan-Saipan clays, 5 to 15 percent slopes; Saipan clay	0.021	59.1	1.24	0.120	0.003
Kagman clay	0.025	88.6	2.22	0.127	0.003
Laolao clay	0.012	29.5	0.35	0.137	0.002
Mesei variant muck	0.001	88.6	0.09	0.108	1.08×10^{-4}
Rock outcrop-Takpochao complex; Takpochao	0.125	6.9	0.86	0.105	0.013
Saipan very gravelly sandy loam	0.001	70.9	0.07	0.113	1.13×10^{-4}
Shioya	0.015	88.6	1.33	0.068	0.001
SUM TOTAL	1.00	--	19.25	--	0.121

for the linear evapotranspiration model. Minimum recharge, when runoff and soil-moisture storage capacity are maximized, was estimated to be 23 in/yr for the step evapotranspiration model.

GROUND-WATER FLOW SYSTEM

Ground water is recharged by rainfall infiltration over most of the island. Water that recharges the ground-water system flows from zones of higher to lower hydraulic head, as measured by water levels in wells. Water-level data indicate that ground water flows radially from the north-central highland and the southeastern ridge and flows generally oceanward. Most of the fresh ground water that is not withdrawn from wells discharges naturally from the aquifer at subaerial and submarine coastal springs. A small amount of ground water may be lost to evaporation and transpiration at Marpo Marsh and Hagoi Lake.

Fresh ground water forms a lens-shaped freshwater body called a freshwater lens, floating on denser seawater within the aquifer. The Ghyben-Herzberg relation commonly is used to relate the thickness of a freshwater lens in an ocean-island aquifer to the density difference between freshwater and saltwater under hydrostatic conditions. Assuming a specific gravity difference of 0.025, a theoretical interface between freshwater and saltwater will be at a depth below sea level that is 40 times the height of the water table above sea level (Todd, 1980). Instead of a sharp freshwater/saltwater interface, however, freshwater is separated from saltwater by a transition zone in which salinity grades from freshwater to saltwater (fig. 6). In many field studies, the theoretical Ghyben-Herzberg interface depth has

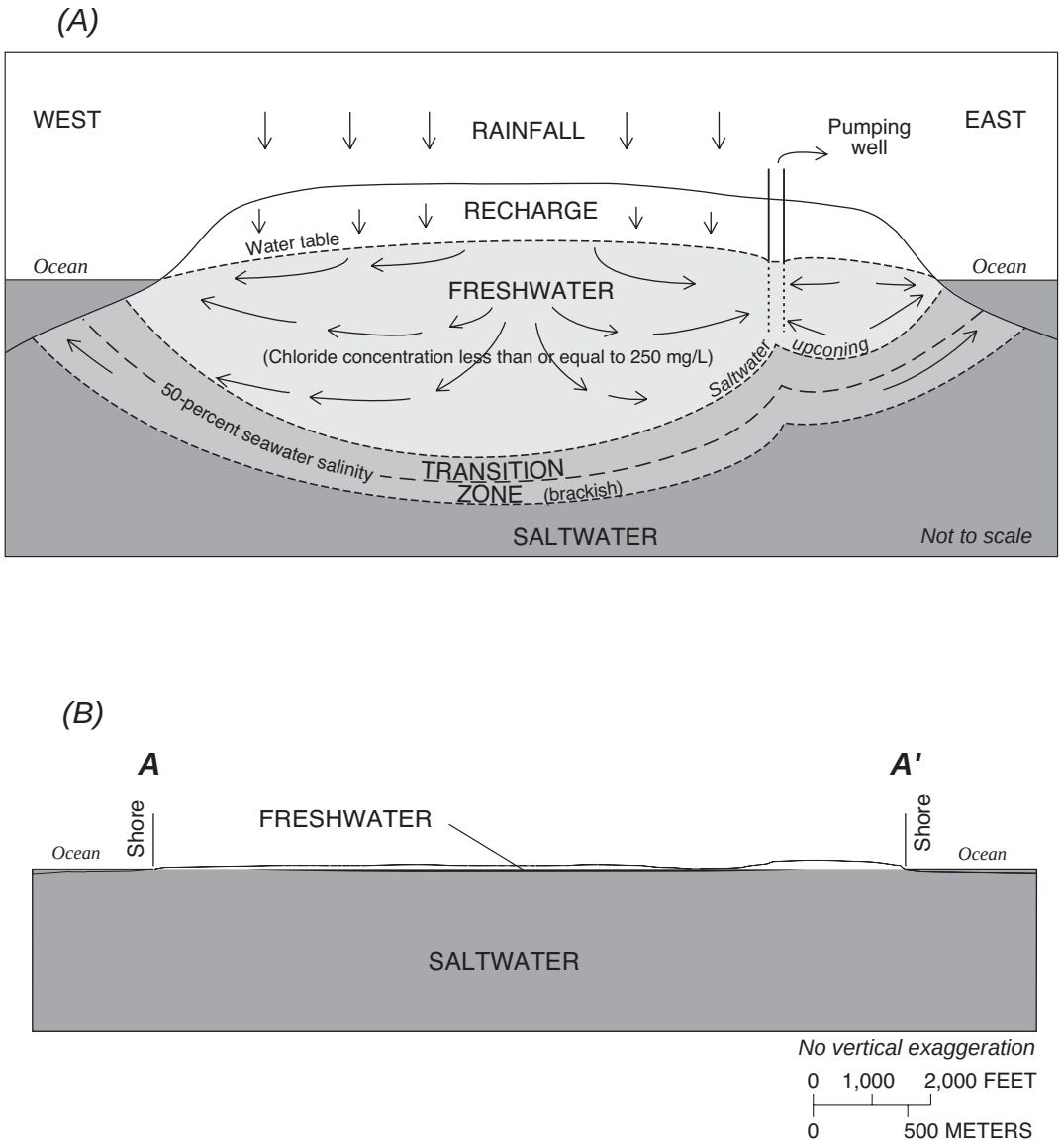

Figure 6. Diagrams of freshwater lens. (A), Schematic diagram of salinity structure and ground-water flow pattern, vertical dimension greatly exaggerated, (B), Tinian freshwater lens, no vertical exaggeration. Line of section shown in figure 1.

been found to correspond to the depth of about a 50-percent mix of freshwater and saltwater. Under equilibrium flow conditions in permeable aquifer systems, the Ghyben-Herzberg relation may provide a reasonable estimate of freshwater depth if the transition zone is comparatively thin.

Freshwater-lens thickness is affected by aquifer permeability and recharge rates. A reduction in recharge rate or an increase in permeability will reduce the height of the water table, which will cause the freshwater lens to be thinner. In the most permeable limestone, the water table is no more than a few feet above sea level, and the slope of the water table is nearly flat.

On Tinian, the freshwater-lens system is in limestone and volcanic rocks but the most important sources of ground water are from the freshwater parts of this system in the limestone rocks. Water levels in well TH19 (fig. 7) indicate that the freshwater lens is in low-permeability volcanic rocks and a vertically extensive freshwater-lens system extends from below sea level to a water table that is tens of feet or more above sea level. Where the low-permeability volcanic rocks cause

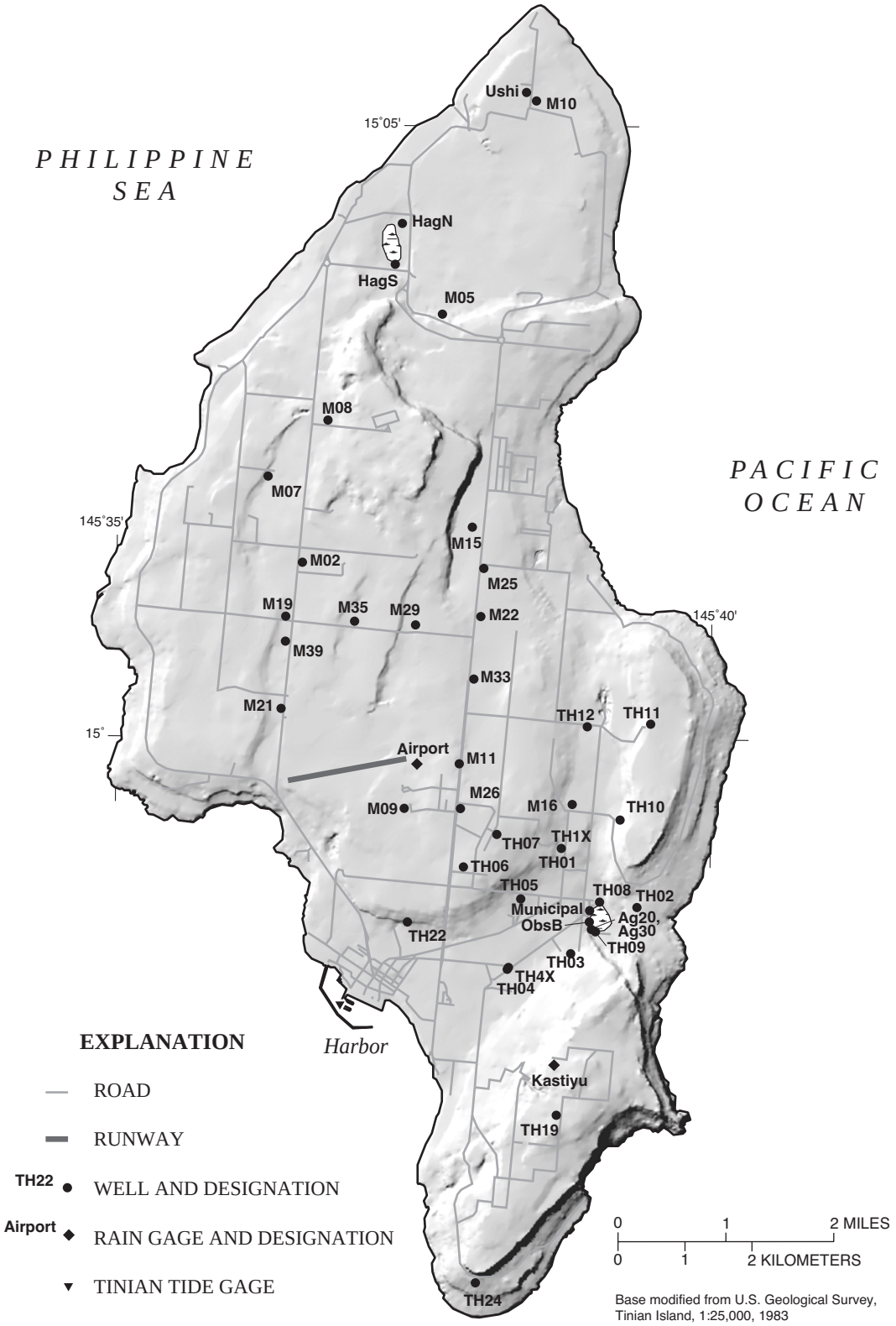

Figure 7. Location of selected wells and rain gages, Tinian.

significant vertical hydraulic-head gradients, the Ghyben-Herzberg principle does not accurately predict the depth where the brackish water in the transition zone has a salinity about 50 percent of seawater. Although reliable water levels and the depth to saltwater have not been measured in wells in these rocks, where flow is downward, the freshwater lens is likely thinner than predicted by the Ghyben-Herzberg principle.

Salinity in a freshwater lens is gradational, from an upper freshwater core through the underlying transition zone to saltwater. On small islands, mixing in the transition zone results mainly from tidal fluctuations superimposed on the gravity-driven flow of freshwater toward the shore. In areas near the coast where mixing is thorough, a freshwater lens may not form and brackish water may exist even at the water table. Under conditions of steady recharge, no pumping, and no ocean-level effects, the steady-state lens would have a fixed size. In reality, rainfall is episodic and seasonal, and lens volume fluctuates naturally with time. Tidal fluctuations, time-varying recharge, and episodic pumping all combine to create a thicker transition zone than would be present without these influences (Underwood and others, 1992).

GROUND-WATER DATA

Available information about the ground water on Tinian includes ground-water withdrawal, ground-water level, and chloride-concentration data. This information has been described in Gingerich and Yeatts (2000).

Withdrawals

The Municipal well (fig. 7), a 300-ft long horizontal trench, supplied all the municipal water for Tinian from 1945 until 1999 when two additional vertical wells (TH04 and TH06) were added to the supply system. From 1990–97, ground-water withdrawal from the Municipal well averaged about 780 gal/min and fluctuated by about 10 percent throughout a year (fig. 8). Fluctuations in withdrawal are related to changes in system conditions or design, pump efficiencies, and water demand. Pumps are generally operated at maximum capacity 24 hours per day, except when one or more pumps are turned off for maintenance or during periods of lower demand in the wet season. In early 1999, wells TH04 and TH06 were put into operation. Well TH06 is capable of producing about 60 gal/min and well TH04 can produce about 50 gal/min. These wells are used during peak demand hours to maintain pressure in the distribution system (Greg Castro, CUC Deputy Director, oral commun., 1999).

A shallow, 30-ft diameter well (well Ag30) was used seasonally to supply irrigation water to cooperative farms, and was usually operated for about 10 hours on alternate days of the dry season. When in use, withdrawal from the irrigation well was estimated to be about 500 gal/min. Use of this well stopped in the mid-1990's. Two other wells that have been in use are wells M25 and M26. These wells were rehabilitated in 1987 by a private corporation and are each pumped at about 25 gal/min for ranch uses.

In 2000–2001, a new 400-ft long infiltration gallery was constructed near the Municipal well (fig. 7). This new infiltration gallery will replace the Municipal well, which will then be used as a backup source. The new infiltration gallery will supply about 875 gal/min (Greg Castro, CUC Deputy Director, oral commun., 2001). Four vertical wells (M19, M21, TH10, and TH12) are also expected to be used in the future.

Water Levels

Changes in ground-water level on an island can reflect changes in recharge or withdrawal from the ground-water system as well as natural changes in ocean level over hourly to yearly time scales. Ground-water flow rates and directions are difficult to determine and are usually inferred from the spatial distribution of water-levels measured at nearly the same time.

Temporal Variation

The most obvious changes in water level occur in response to the ocean tide (fig. 9). The daily ground-water level response to the ocean tide is attenuated as it travels through the aquifer, decreasing with increasing distance from the ocean. The daily water-level changes in the Ushi well, 2,790 ft from the coast, averaged about 0.5 ft and the Municipal well, 4,080 ft from the coast, had daily water-level changes that averaged about 0.15 ft. Well M21, at 4,690 ft from the coast, had daily fluctuations that averaged about 0.01 ft. Three other wells (M02, M29, and TH07) that were monitored continuously by the USGS showed no daily tidal

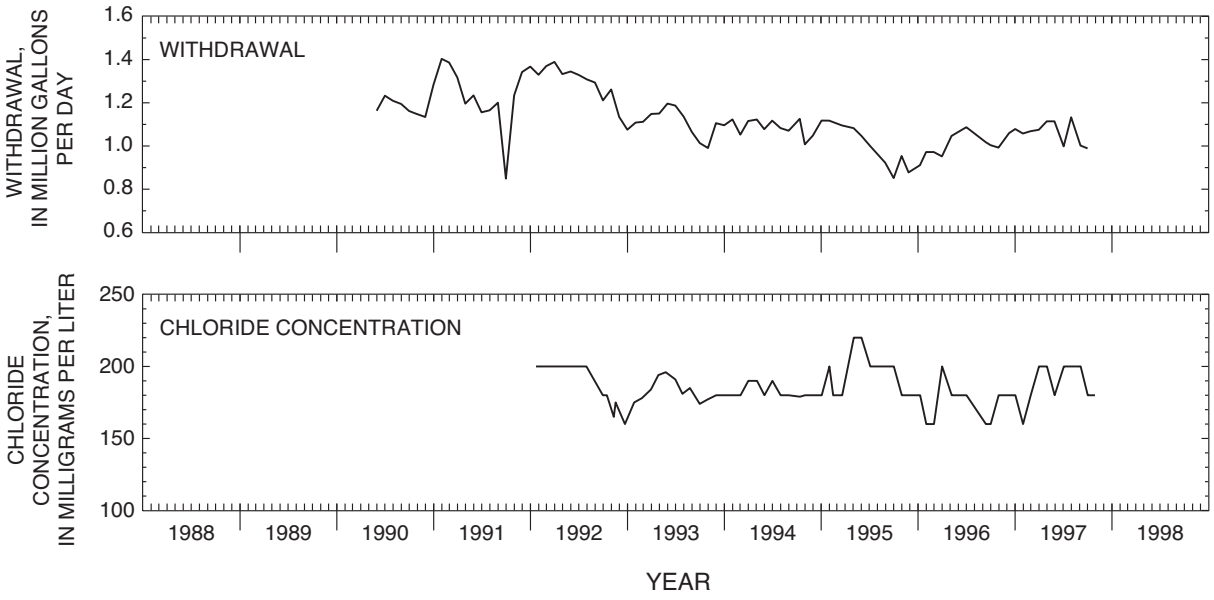

Figure 8. Ground-water withdrawal and chloride concentration at Municipal well, Tinian (Source: Greg Castro, CUC Deputy Director, oral commun., 1998).

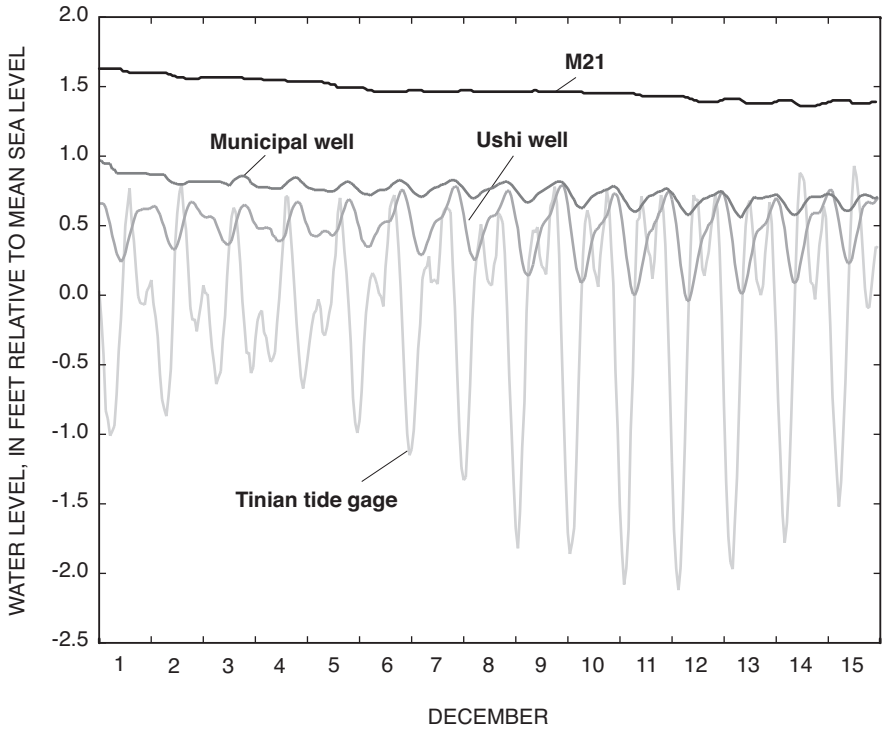

Figure 9. Selected ground-water levels and ocean level, Tinian, December 1–15, 1992.

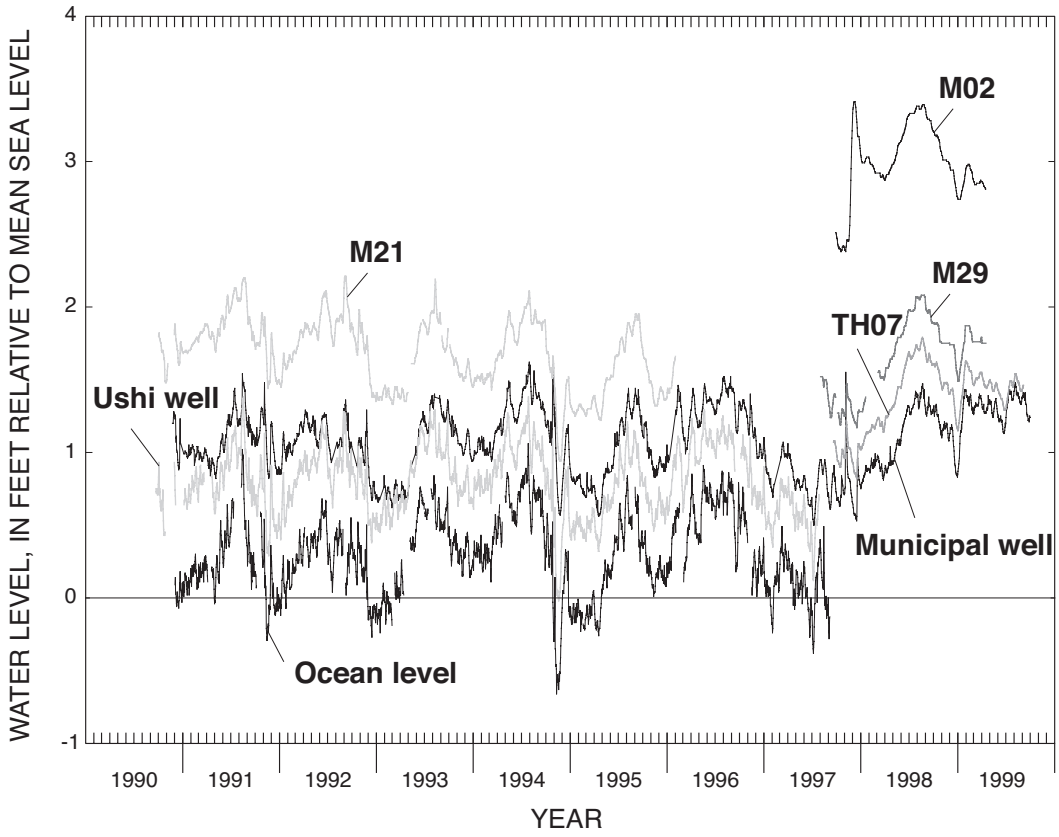

Figure 10. Ground-water levels and ocean level, Tinian, 1990–99.

fluctuations; these wells are 7,660 ft, 9,630 ft, and 9,430 ft from the coast, respectively.

In addition to the daily fluctuation in water level caused by the ocean tides, water levels in wells also vary over longer times in response to non-periodic changes in ocean level and to rainfall (fig. 10). During the entire period that the tide gage (fig. 9) was operating (1990–97), the ocean-level record with the tidal fluctuations removed ranged from -0.7 ft to 1.2 ft altitude. The water-level records with the tidal fluctuations removed from the Ushi and Municipal wells show variations that correspond closely to the ocean-level record. Although the tide gage was discontinued in 1997, it is apparent that wells M02, M21, M29, and TH07 also respond to the ocean level because the water-level records from these wells are similar to the Municipal well water-level record which is the expected response to low-frequency variations in ocean level.

The difficulty in determining the effects of recharge and withdrawal on water levels is illustrated in figure 10. For example, the decline in water level of nearly 0.7 ft in the Ushi well during January to March 1997 may be due mainly to the decline in ocean level and cannot be conclusively attributed to a decline in recharge during the annual dry season. With the exception of the water-level record from well M02, all of the variations in water level in the monitored wells appear to be directly in response to variations in ocean level with slight additional variation because of heavy rainfall. The effects of changes in recharge or withdrawal cannot be readily evaluated using these water-level records. The water-level rise of nearly 1 ft in well M02 during the end of December 1997 does not correlate with any of the other concurrent water-level records. The cause of this increase is unknown but may be from recharge after an episode of heavy rainfall combined with the effects on ground-water flow caused by nearby low-permeability volcanic rocks.

Spatial Distribution

The water table defines the top surface of the freshwater lens. Water-table contours for July 4, 1997 (fig. 11) show two mounds in areas where low-permeability pyroclastic rocks are above sea level and a localized zone of water-table depression near the Municipal well, which was withdrawing water at the time of the measurements. Details of the data collection and preparation of this map are described in Gingerich and Yeatts (2000). Over most of the island, the water table is relatively flat and water levels are less than 2 ft above mean sea level.

Water-level measurements made on other dates help constrain where water-level contours are drawn. The highest measured water level in the limestone was 3.42 ft above mean sea level on December 7, 1997 in well M02, which is directly west of the north-central highland. The highest measured water level on the island was in the pyroclastic rocks on the southeastern ridge where water level was about 90 ft above mean sea level on May 29, 1997 in well TH19. The water table is expected to be similarly high in the pyroclastic rocks of the north-central highland but no wells are available there to provide water-level data.

The water-table shape can be used to infer directions and rates of ground-water flow as well as the movement of contaminants dissolved in the flowing ground water. In an isotropic aquifer, fresh ground water will flow from areas of higher water level to areas of lower water level, in directions roughly perpendicular to the water-table contours (fig. 11). The water-table contours indicate that ground water moves radially from the north-central highland and the southeastern ridge and flows generally oceanward or toward production wells.

The water-table map reflects pumping conditions in the aquifer because withdrawal from the Municipal well had been steady during the preceding months (fig. 8). Drawdown from pumping diverts some of the oceanward ground-water flow to wells. To what degree the water-table configuration represents the long-term average configuration is not known. A long-term average configuration could be determined by operating continuous water-level recorders at numerous wells and averaging the data over the desired time, such as a year, assuming ground-water withdrawals are constant.

Chloride Concentration

Chloride concentration is generally used as an indicator of saltwater intrusion into the ground-water system. In general, chloride concentrations are expected to increase with depth in the aquifer and proximity to the ocean but exceptions can exist because of local-scale heterogeneities in the aquifer. In a thin freshwater lens, the chloride concentration of water pumped from a well may increase with increasing pumping rate.

Vertical Distribution

The thickness of the potable part (less than or equal to 250 mg/L) of the freshwater lens beneath the median valley (fig. 1, A-A′) is shown in a vertical section (fig. 12). Details of the preparation of the vertical sections are described in Gingerich and Yeatts (2000). The section shows that the freshwater lens is thickest in the center of the island near well TH04 and thins toward the east and west coasts. The maximum thickness attained by the freshwater in this section is about 40 ft. The freshwater lens is slightly thinner in the east than in the west, which indicates saltwater may be upconing in the east because of ground-water withdrawal at the Municipal well and evapotranspiration at the Marpo Marsh.

Changes in the freshwater-lens thickness are generally seasonal. The lens thickens after the wet season and thins after the dry season. After an average wet season (1993), the midpoint of the transition zone was about 3 to 5 ft deeper than the previous position indicating that the freshwater lens had become slightly thicker (Gingerich and Yeatts, 2000). During the following dry season, which was wetter than average, the freshwater-lens thickness decreased only slightly (1 to 2 ft) in response to a decrease in recharge. After a dry season of more typical rainfall, the lens would be expected to shrink to a greater extent.

Temporal Variation in Pumped Water

The chloride concentration at the Municipal well did not change significantly during 1992–97, averaging about 180 mg/L, and ranging from 160 to 220 mg/L. Chloride concentration was usually slightly lower in the wet season as compared to the dry season. The average chloride concentration is about 100 mg/L higher than initially measured during non-pumping conditions after construction in 1945 (Lawlor, 1946), and 100 mg/L higher than at other wells in the median valley. Monitor wells TH08, TH09, and TH03 are near the Municipal

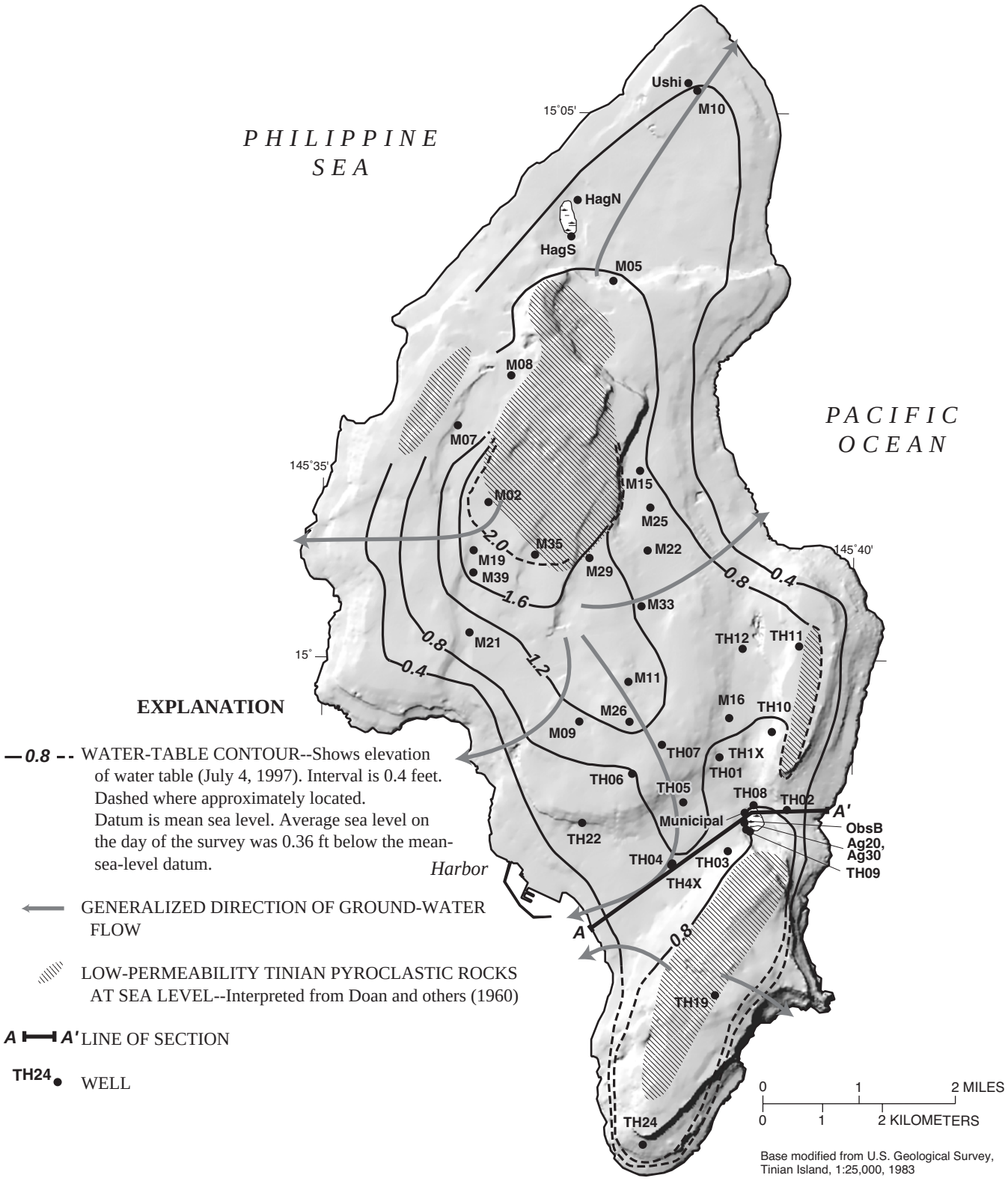

Figure 11. Configuration of the water table, July 4, 1997, Tinian. (from Gingerich and Yeatts, 2000).

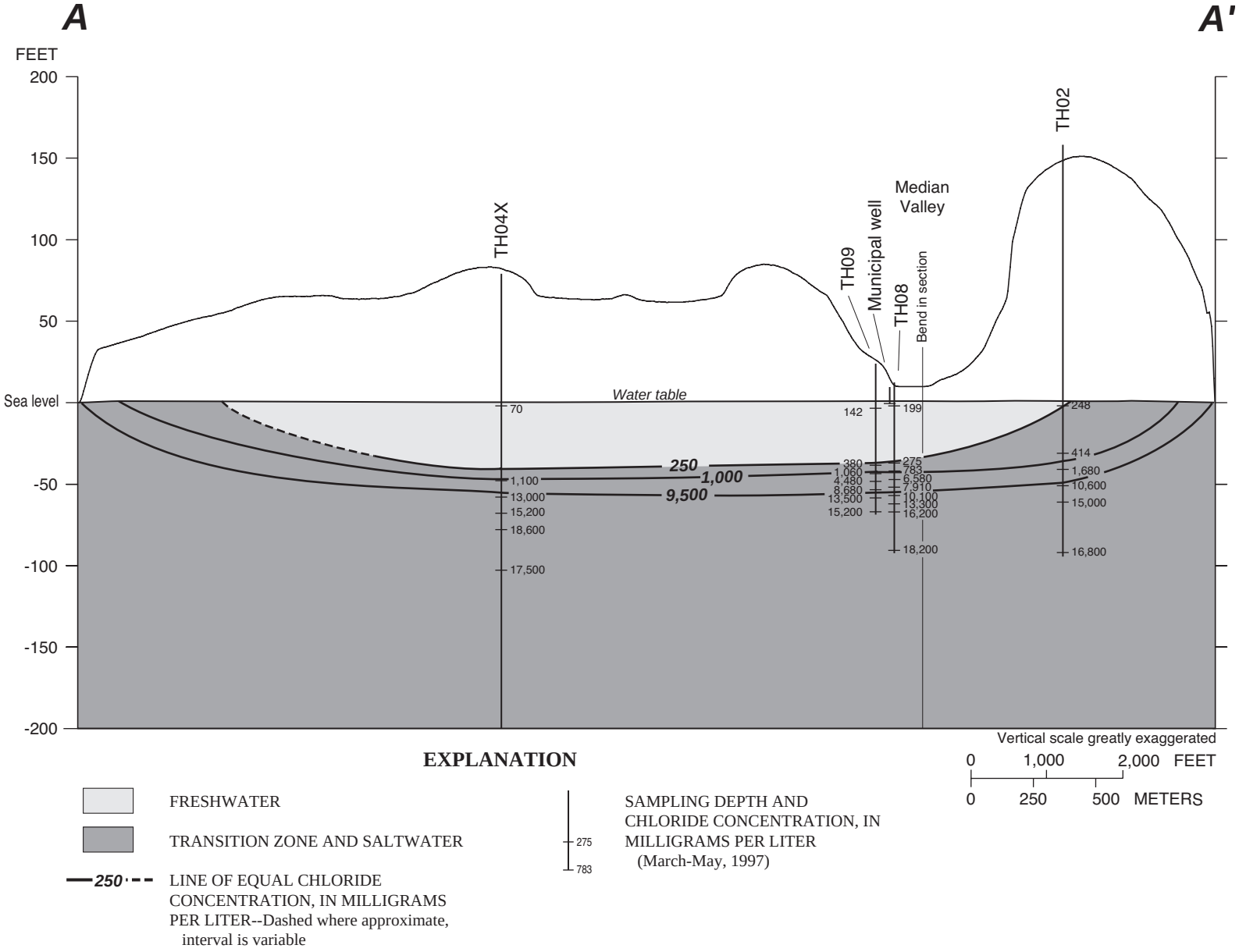

Figure 12. Thickness of freshwater lens (to a depth of 250 mg/L chloride concentration) and upper transition zone, Tinian, March 5–6 and May 23, 1997 (Gingerich and Yeatts, 2000). Line of section is shown in figure 11.

well and show similar chloride concentrations, near 180 mg/L, indicating that the chloride concentration at these wells may be elevated as a result of pumping at the Municipal well.

DEVELOPMENT OF STEADY-STATE GROUND-WATER FLOW MODEL

A two-layer (areal), ground-water flow model using the computer code SHARP (Essaid, 1990) was developed to simulate steady-state ground-water flow on Tinian. The SHARP code uses a finite-difference approach to simulate flow in a ground-water system containing both freshwater and saltwater and treats freshwater and saltwater as immiscible fluids separated by a sharp interface. In reality, a diffuse transition zone exists between the freshwater and underlying saltwater. In this study, it is assumed that the position of the surface defined by ground water with 50-percent seawater salinity is approximated by the sharp-interface position. The SHARP code simulates vertically averaged freshwater heads and vertically averaged saltwater heads in the aquifer and assumes that flow within each model layer is entirely horizontal.

The model accounts for spatially varying hydraulic characteristics of the geologic materials and ground-water withdrawals. The hydraulic characteristics were estimated from available data and modified by varying them in the model to obtain acceptable agreement between measured and model-calculated water levels.

Model Grid

The finite-difference grid used consists of two layers, each having 4,450 cells arranged in a rectangular array with 89 rows and 50 columns (fig. 13). The northwest grid corner is at longitude 145°32′42″W and latitude 15°08′02″N and the long side of the grid is oriented north south. The active part of the grid extends at least 3,700 ft offshore to include the entire zone where fresh ground water discharges to the ocean. Grid spacing across the island is uniform with each cell having square sides 820 ft long. Offshore cells near the grid perimeter, where freshwater flow is not expected, were larger.

Boundary Conditions

Two types of boundary conditions were used in the model, specified flow (which includes no flow) and head-dependent discharge. The outer rows and columns of the grid and the aquifer bottom are treated as no-flow boundaries. The aquifer bottom was assumed to be 5,000 ft below sea level onshore and offshore. In each cell, the base of the top layer was set equal to (1) the top of the volcanic rocks where the top of the volcanic rocks were below sea level or (2) sea level where the volcanic rocks were above sea level (fig. 14). All cells in the top layer representing offshore areas were modeled using a head-dependent discharge boundary condition. All cells in the top layer not simulated as a head-dependent discharge boundary represented aquifer materials that were simulated under unconfined conditions in the model.

Freshwater flow (Q) out of the model at head-dependent discharge cells is assumed to be linearly related to the difference between the head in the aquifer (h) and the head overlying the aquifer (h_0) at the discharge site according to the equation:

$$Q = (K'/B')A(h-h_0) \qquad (8)$$

where:

Q = rate of discharge from a model cell [L^3/T],
K' = vertical hydraulic conductivity of the confining unit overlying the aquifer [L/T],
B' = thickness of the confining unit overlying the aquifer [L],
A = area of the model cell [L^2],
h = head in the aquifer [L], and
h_0 = head above the aquifer, measured relative to mean sea level [L].

The confining-unit vertical hydraulic conductivity divided by the confining-unit thickness is termed the coastal leakance in this report. Although a low-permeability coastal confining unit does not exist around Tinian, the limestone itself impedes ground-water discharge to the ocean. Thus, the confining-unit vertical hydraulic conductivity is represented by the limestone vertical hydraulic conductivity and the confining-unit thickness is represented by the aquifer thickness through which vertical discharge occurs. No attempt was made to estimate separate values for the aquifer thickness through which vertical discharge occurs and the vertical hydraulic conductivity; instead

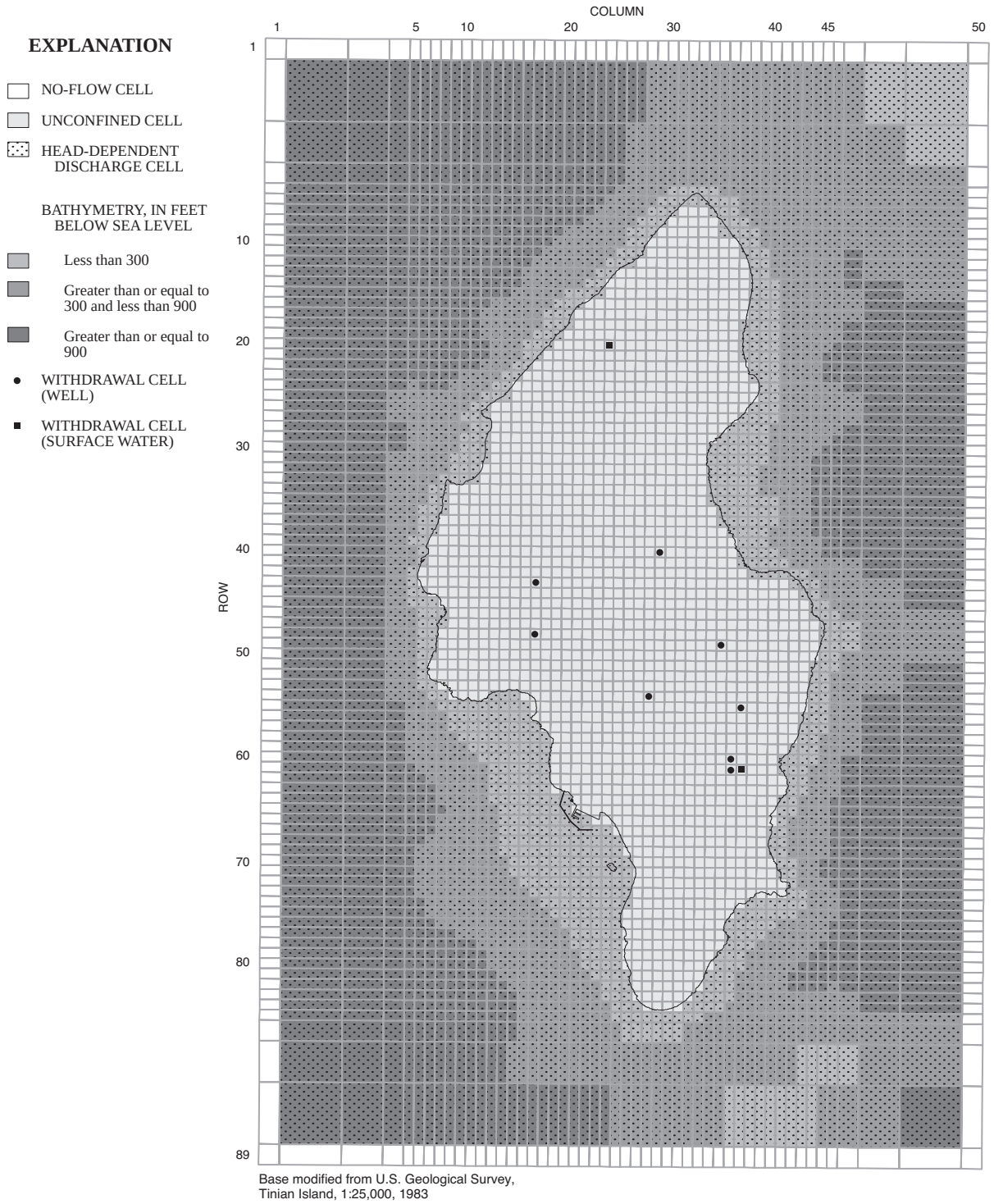

Figure 13. Finite-difference model grid, head-dependent discharge cells, and withdrawal cells for Tinian ground-water flow model.

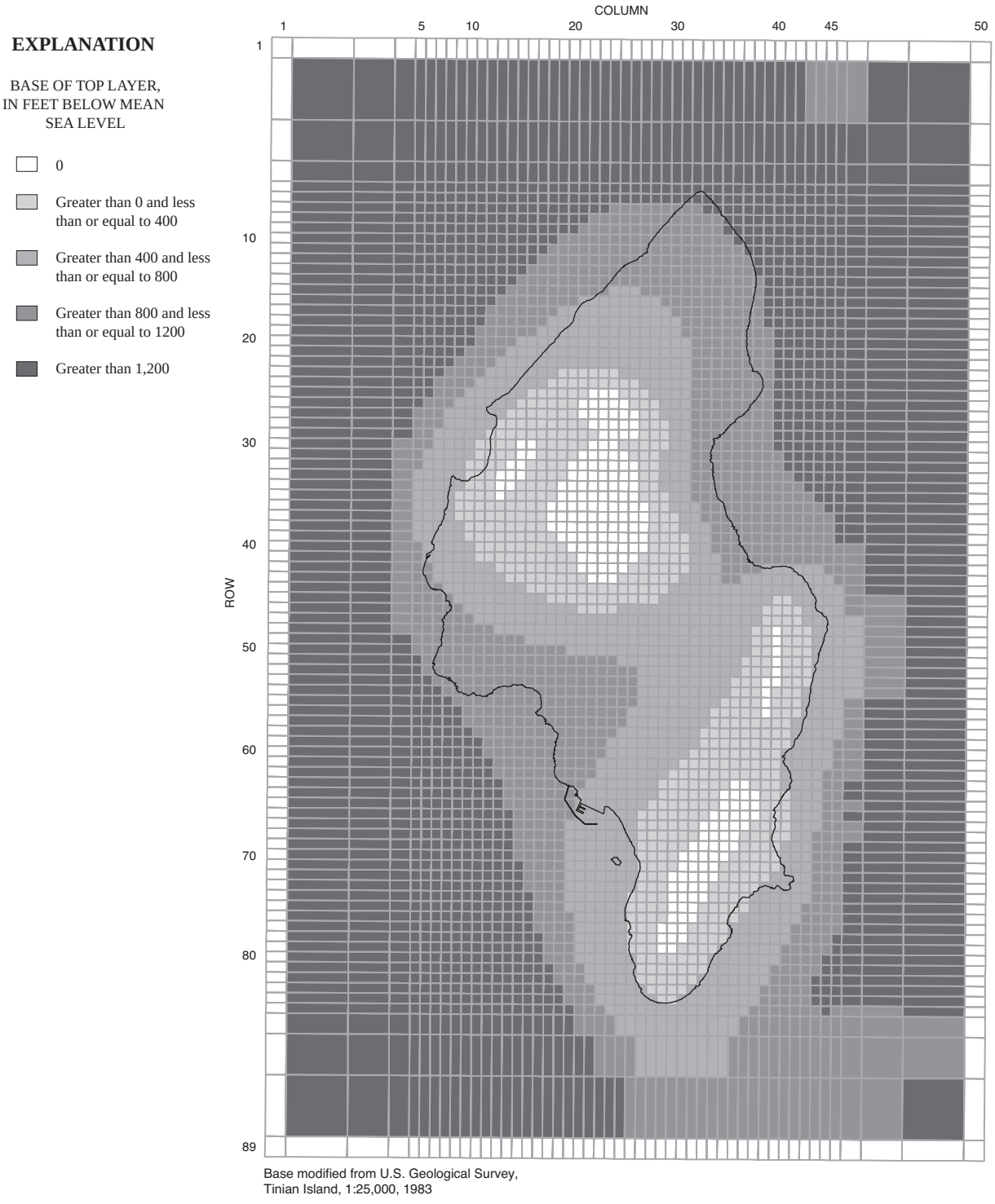

Figure 14. Finite-difference model grid and base of top layer for Tinian ground-water flow model.

the coastal leakance was assumed to be 10 day^{-1} throughout the grid. This high value of leakance was used so that ground water in the model could freely discharge to the ocean as controlled by the horizontal hydraulic conductivity of the aquifer and heads would not build artificially in response to a leakance controlled by the vertical hydraulic conductivity of the aquifer.

The head (h_0) overlying the aquifer offshore was assigned a value corresponding to the freshwater-equivalent head of the saltwater column overlying the ocean floor within the cell. The freshwater-equivalent head, measured relative to mean sea level, was computed from the equation:

$$h_0 = -Z/40 \quad (9)$$

where Z is the ocean-floor altitude.

Flow between lower and upper layers of the model is a function of the difference in head between the layers and the value of leakance between the layers. This flow can also be represented by equation 8 assuming the leakance and head-difference terms represent values for leakance and head difference between the lower and upper layer. Thus, the confining-unit vertical hydraulic conductivity is represented by the vertical hydraulic conductivity of the limestone or volcanic rocks and the confining-unit thickness is represented by the aquifer thickness over which vertical flow occurs.

Because the saturated thickness of each cell changes with the water-table elevation and depth to the interface between saltwater and freshwater as the SHARP code iterates to a solution, so too should thickness and leakance values. The original version of SHARP (Essaid, 1990) does not recalculate these values so a modified version of the SHARP code (Izuka and Gingerich, 1998), which automatically recalculates leakance as thickness changes, was used to create the Tinian model.

Hydraulic Conductivity Zones

Tinian was divided into three horizontal hydraulic-conductivity zones (fig. 15): (1) highly permeable limestone (hydraulic conductivity = 10,500 ft/d), (2) less-permeable limestone (hydraulic conductivity = 800 ft/d), and (3) low-permeability volcanic rocks (hydraulic conductivity = 0.2 ft/d). The less-permeable limestone zone was simulated to adequately represent the area of higher water levels (wells M02, M19, M35, and M39) to the southwest of the north-central highland. The lack of tidal response in water levels from well M02 and the relatively low permeability estimated from the aquifer test at well M19 support this zonation.

Recharge

The recharge value used in the model was 30 in/yr, an average of the two water-budget accounting methods (see Water Budget section). Recharge was distributed uniformly across the island to produce an equivalent recharge of 54.9 Mgal/d.

Ground-Water Withdrawals

Ground-water withdrawal was represented using pumping cells in the ground-water model. Six pumping cells, four that represent wells, were used for the steady-state model, which matches conditions during 1990–97 (table 4, pumping scenario A, the base-case scenario). Evaporation from the water table at Hagoi Lake and Marpo Marsh is also represented with pumping cells. Annual evaporation was estimated by multiplying the mapped area of the water body by the annual pan-evaporation rate (76.65 in/yr on Guam [1956–82]) and multiplying the results by 0.7, the pan-evaporation coefficient typically assumed to convert pan evaporation to lake evaporation (see, for example, Dunne and Leopold, 1978; Linsley and others, 1982). Total simulated ground-water withdrawal from wells was 854 gal/min or about 2 percent of the total estimated recharge to the island.

Water Properties

The specific weights for freshwater and saltwater were assumed to be 62.41 lb/ft^3 and 63.97 lb/ft^3, respectively (Essaid, 1990). Hydraulic conductivity is dependent on fluid viscosity, which in turn is a function of temperature, and to a lesser extent pressure and salinity. The freshwater and saltwater dynamic viscosities used in the model were 2.09×10^{-5} $lb \cdot s/ft^2$ and 2.24×10^{-5} $lb \cdot s/ft^2$ (Weast and others, 1989), respectively, for an assumed temperature of 20°C.

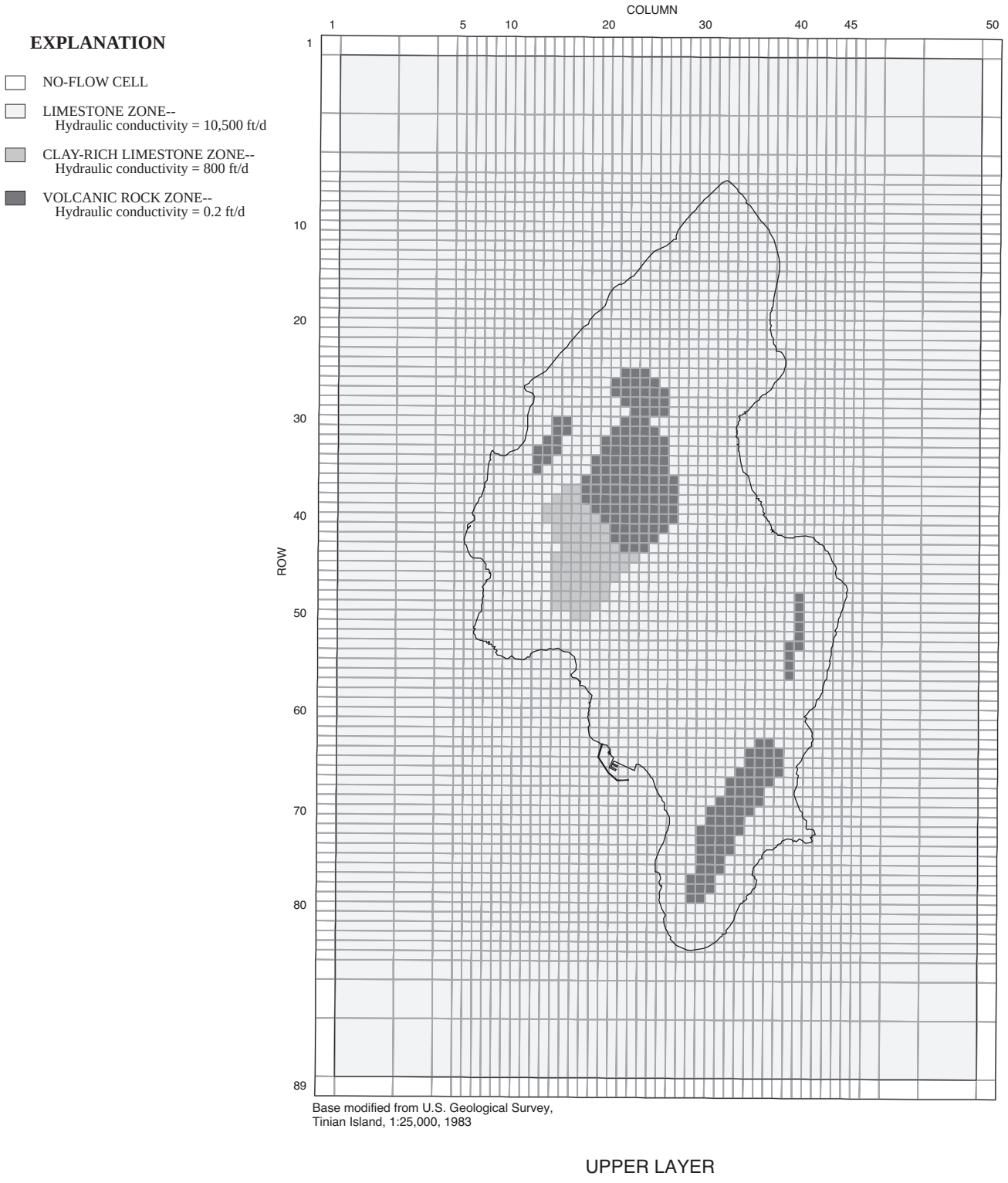

Figure 15. Finite-difference model grid and hydraulic-conductivity zones for Tinian ground-water flow model.

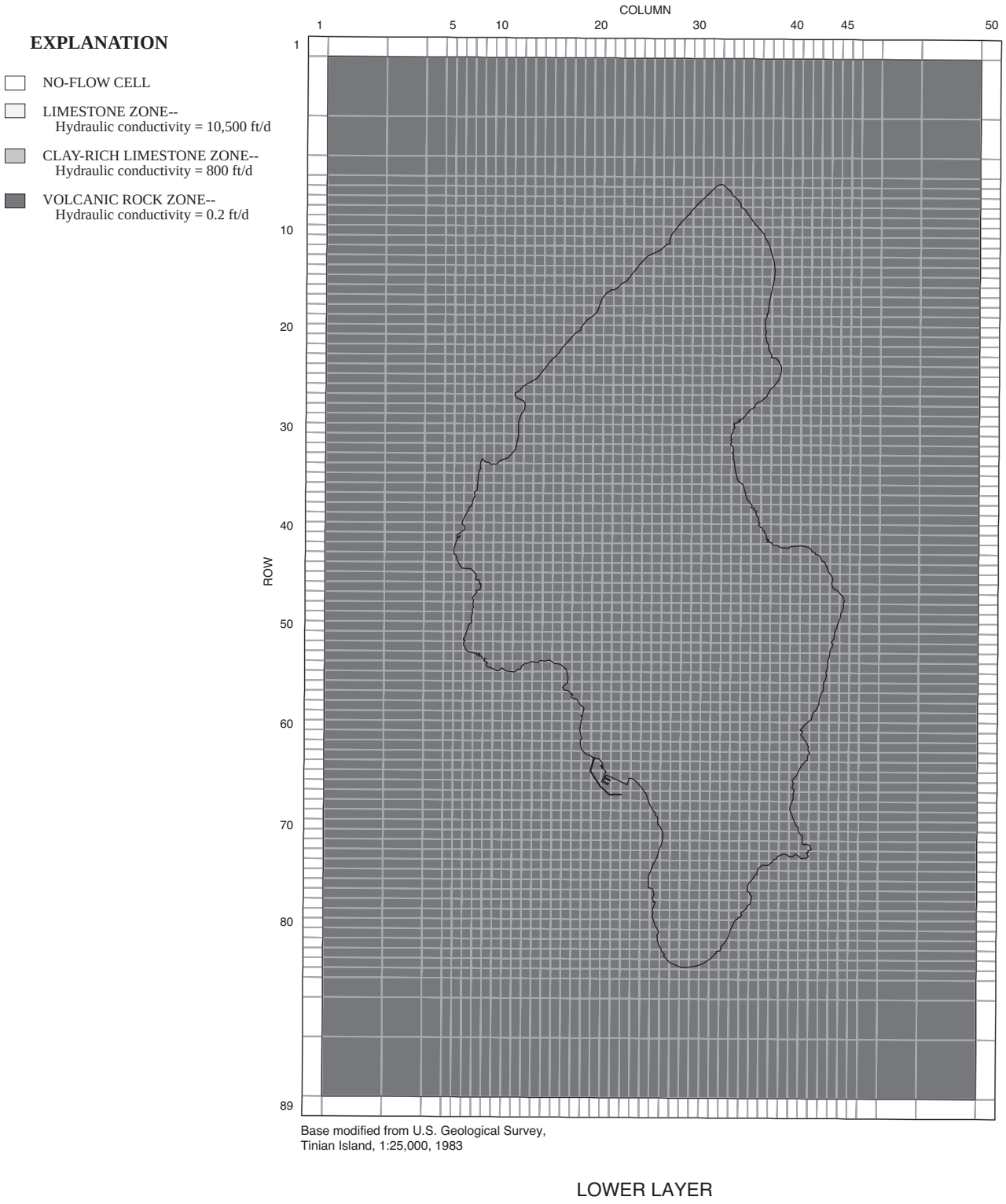

Figure 15. Finite-difference model grid and hydraulic-conductivity zones for Tinian ground-water flow model.--Continued

Table 4. Description of pumped well sites and reported pumping rates, Tinian

[gal/min, gallons per minute; pumpage from water bodies represents pumpage equivalent to evaporative loss; pumping scenarios are: A, average pumping distribution from 1990–97 (base-case scenario); B, no pumping; C, 2001 pumping distribution; D, maximum pumping distribution]

Wellsite name	Altitude of top of open interval (feet)	Altitude of bottom of open interval (feet)	Model cell (row, column)	Steady-state pumping rate (gal/min)	Pumping scenario in which well was simulated
Municipal well	9	-2	60, 36	780	A, D
New municipal well	5	-2	61, 36	875	C, D
Ag30	1	-5	61, 36	26	A, D
M19	5	-14	43, 17	50	D
M21	5	-17	48, 17	50	D
M25	5	-88	40, 29	25	A, D
M26	5	-30	54, 28	23	A, D
TH04	51	-18	64, 31	50	C, D
TH06	8	-12	58, 28	50	C, D
TH10	154	-16	55, 37	50	D
TH12	136	-12	49, 35	50	D
Hagoi Lake[a]	1	0	20, 24	29	All
Marpo Marsh[a]	1	0	61, 37	86	All

[a]evaporation simulated using a withdrawal well

Estimation of Hydraulic Characteristics and Model-Calculated Water Levels

Values of horizontal hydraulic conductivity for the numerical model were varied until simulated water levels at specified monitoring points matched measured water levels. Recharge, ground-water withdrawal, and coastal leakance were held constant. Because the model simulated steady-state conditions with constant recharge and withdrawal, average measured water levels can be used as targets for the model simulations. Measurements made at different times cannot always be compared directly because water levels on Tinian vary with the ocean level. To provide comparable water-level measurements, values were adjusted up or down using the Municipal well record as an index record. The Municipal well water-level record was recorded continuously during November 1990 to April 1999 and is the longest water-level time series available (fig. 10). Water levels from each well were adjusted using the following procedure:

1) Determine the period over which water-level measurements were made in the well.

2) Average the water levels over that same period in the Municipal well.

3) Determine the difference between that water level and the average Municipal well water level over the entire period.

4) Subtract the difference from the average water level of the well in question to determine the adjusted water level.

For example, during the period over which well M21 was monitored (September 30, 1990 to February 1, 1996), the Municipal well water level averaged 1.06 ft above the sea level datum, or 0.03 ft above the average of 1.03 ft during the entire period of record (table 5). The adjustment of 0.03 ft was subtracted from the average water level in M21, 1.65 ft, to obtain an adjusted water level of 1.62 ft above the sea level datum. Water-level records from wells M02 and M29 needed significant but opposite adjustments even though the period of monitoring was about the same. One explanation for this may be because both wells are near the central highlands where lower permeability limestone is expected. Because the rocks in this area have less permeability, changes in water levels may be increasingly affected by recharge and less so by changes in ocean level than water levels in wells penetrating the highly permeable limestone.

Table 5. Observed and model-calculated water levels used in the steady-state simulations, Tinian

[All water-level measurements are intermittent unless otherwise noted]

Well name	Average measured water level (feet above mean sea level)	Number of measurements	Period when measurements were collected	Difference in Municipal well water level during measurement period and entire period (feet)	Adjusted water level (feet above mean sea level)	Model-calculated water level (feet above mean sea level)
M02[a]	2.89	15,700	9/25/97-4/16/99	0.24	2.65	2.62
M05	0.69	3	7/31/97-10/1/97	-0.24	0.93	1.07
M07	1.46	25	7/6/95-10/1/97	0.08	1.38	1.51
M08	1.02	3	8/22/97-10/3/97	-0.29	1.31	1.41
M09	1.40	31	5/4/95-10/2/97	0.00	1.40	1.36
M10	0.58	8	3/31/97-12/29/97	-0.26	0.84	0.75
M11	1.63	34	4/13/95-12/29/97	0.00	1.63	1.43
M15	1.02	6	5/29/97-12/29/97	-0.28	1.30	1.19
M16	1.28	32	5/4/95-12/29/97	0.02	1.26	1.36
M19	1.87	5	6/5/97-12/30/97	-0.28	2.15	2.18
M21 [a]	1.65	45,443	9/30/90-2/1/96	0.03	1.62	1.65
M22	1.12	5	7/4/97-12/30/97	-0.26	1.38	1.36
M25	1.36	28	11/1/94-9/5/97	0.00	1.36	1.27
M26	1.75	20	11/1/94-9/5/97	-0.02	1.77	1.39
M29 [a]	1.40	14,524	7/30/97-4/16/99	-0.24	1.64	1.53
M33	1.30	4	8/22/97-12/30/97	-0.28	1.58	1.45
M35	2.16	4	7/31/97-12/30/97	-0.26	2.42	2.58
M39	1.74	7	5/15/97-12/30/97	-0.28	2.02	2.11
Municipal [a]	1.03	67,952	11/22/90-4/16/99	0.00	1.03	1.03
HagN	1.20	39	5/17/93-7/4/97	0.07	1.27	0.90
HagS	1.24	38	5/17/93-7/4/97	0.07	1.31	0.97
TH01	1.12	4	9/17/96-12/29/97	0.01	1.11	1.29
TH02	0.64	5	4/30/97-9/5/97	-0.28	0.92	0.86
TH04	1.32	48	1/10/94-12/29/97	0.02	1.30	1.19
TH06	1.30	27	7/6/95-7/31/97	0.08	1.22	1.30
TH07 [a]	1.28	9,233	9/17/97-4/16/99	-0.01	1.29	1.36
TH09	1.27	114	2/9/93-12/30/97	0.02	1.25	1.07
TH10	1.12	18	10/10/96-12/29/97	-0.15	1.27	1.29
TH12	1.13	10	1/8/97-12/29/97	-0.24	1.37	1.33
TH22	1.06	17	10/31/96-12/29/97	-0.19	1.25	1.05
Ushi [a]	0.81	53,296	10/1/90-7/28/97	0.03	0.78	0.72

[a]continuous-recorder data

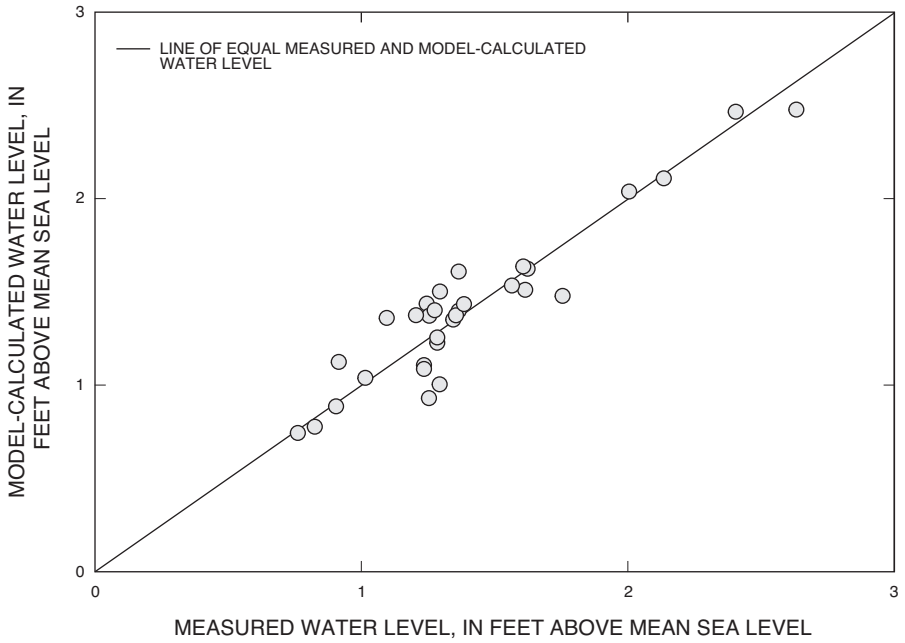

Figure 16. Measured and model-calculated water levels for base-case scenario, Tinian, for a coastal leakance of 10 feet per day per foot, a horizontal hydraulic conductivity of 10,500 feet per day for the highly permeable limestone zone, a horizontal hydraulic conductivity of 800 feet per day for the less-permeable limestone zone, and a horizontal hydraulic conductivity of 0.2 feet per day for the volcanic-rock zone.

Table 6. Final hydraulic-conductivity values used in the groundwater flow model, Tinian

Model zone	Hydraulic conductivity (feet per day)
Highly permeable limestone	10,500
Less-permeable limestone	800
Low-permeability volcanic rocks	0.2

Model-calculated water levels in layer 1, which represent the water-table altitude, were compared with these adjusted water levels to determine the best combination of hydraulic-conductivity values in the model (fig. 15). The final hydraulic-conductivity values used in the model are listed in table 6. The model-calculated water levels are in good agreement with the adjusted measured water levels (fig. 16). The average of the differences, average-absolute value of the differences, and root-mean-square of the differences between measured and model-calculated water levels were 0.01, 0.11, and 0.30 ft, respectively. The model-calculated water levels (fig. 17) show good agreement with the hand-contoured water-table map (fig. 11).

The model-calculated position of the freshwater/saltwater interface can be compared with measured data during 1997 to illustrate how well the model represents the freshwater-lens system (fig. 18). In general, the depth to the position of the surface defined by ground water with a 50-percent seawater salinity (about 9,500 mg/L chloride concentration) measured in 1997 was deeper than the model prediction for average conditions. One explanation for this discrepancy could be that the model-calculated water levels in the area where the measured transition-zone data were collected are slightly lower than measured water levels in the area. No attempt was made to match water levels at each well individually; instead the model simulates the overall shape of the water table and gives equal weight to water-level measurements made throughout the island. It was determined that this matching criteria would be more appropriate than applying more weight to the water-level measurements near where transition-zone measurements were made.

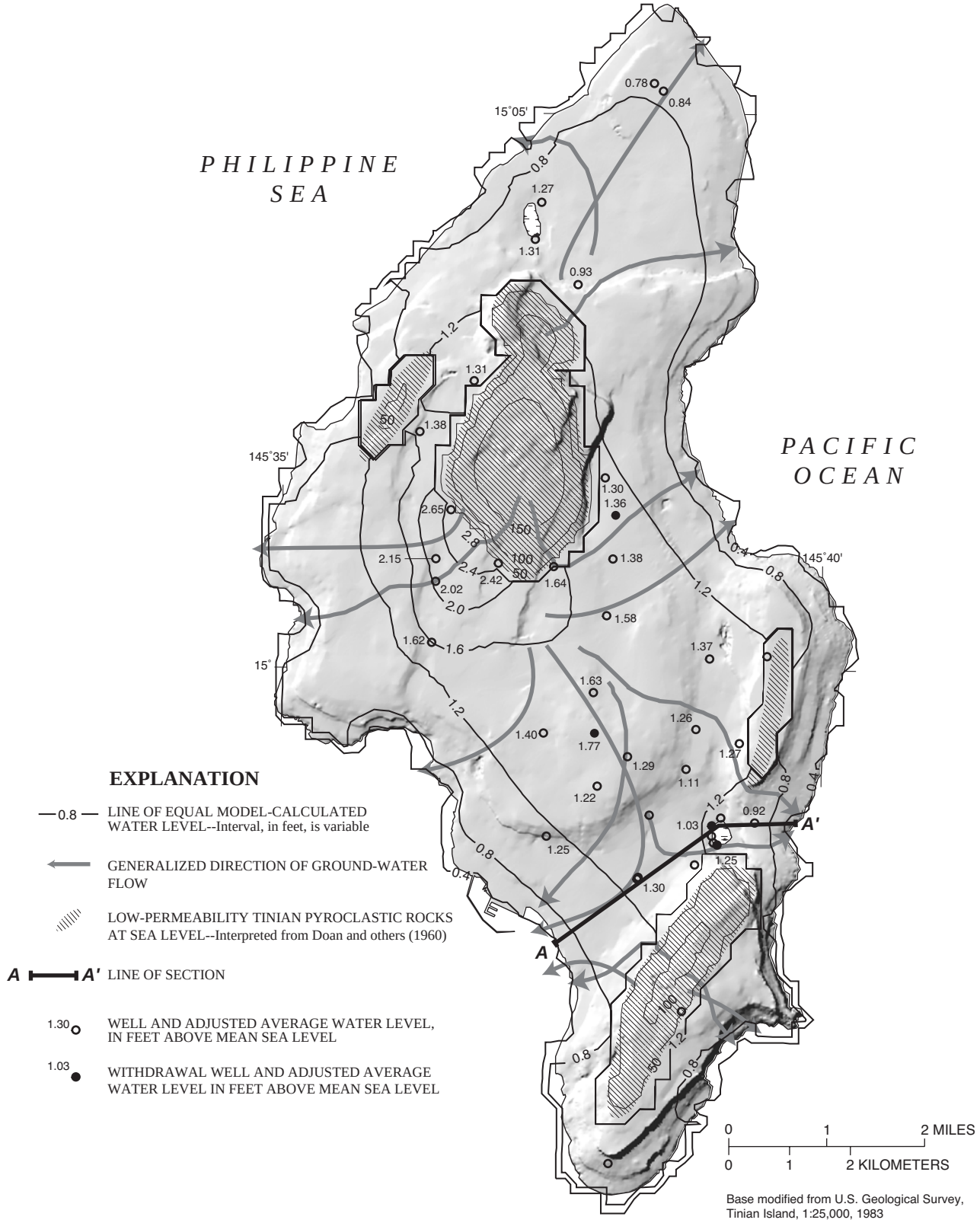

Figure 17. Average measured and model-calculated water levels for base-case scenario, Tinian.

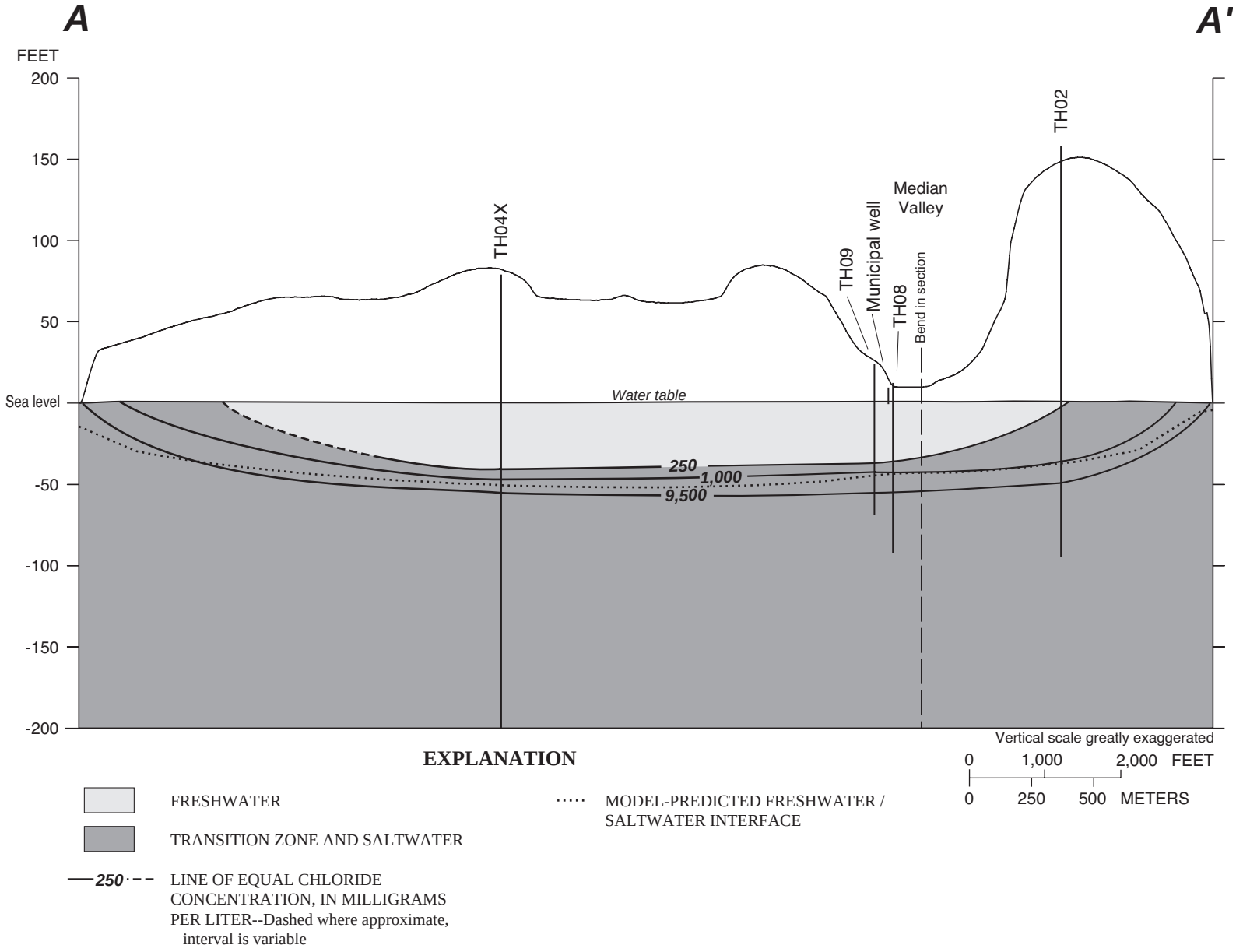

Figure 18. Position of model-simulated interface for base case compared with observed thickness of freshwater lens, Tinian, March 5–6 and May 23, 1997. Line of section is shown in figure 11.

Model Response to Changes in Hydraulic Characteristics

Three sets of simulations were used to determine model sensitivity to changes in hydraulic conductivity of the limestone, volcanic rocks, and coastal leakance. In the first set of simulations, hydraulic conductivity of the limestone was changed by 25 percent above and below the values used in the base-case scenario (table 6). In the second set of simulations, coastal leakance was increased to 100 day^{-1} and decreased to 0.1 day^{-1}. In the third set of simulations, the hydraulic conductivity of the volcanic rocks was increased from 0.2 to 2 and 20 ft/d. Results of these changes are shown as scatter plots in which model-calculated water levels are plotted against measured water levels (fig. 19). Also shown for reference in each scatter plot is the line on which all data would lie if the model-calculated water levels were exactly equal to the measured values. Comparison of results shown in figure 19 indicates that model-calculated water levels are sensitive to changes in limestone hydraulic conductivity of 25 percent but not affected significantly by changes in coastal leakance or volcanic rock hydraulic conductivity of an order of magnitude.

Although the sensitivity of the base-case model to changes in the estimates of annual recharge was not evaluated, these changes would have essentially the same effect as varying the limestone hydraulic conductivity. A 25-percent increase in the limestone horizontal hydraulic conductivity throughout the island will have essentially the same effect on water levels as a 25-percent decrease in recharge to the island. Similarly, a decrease in limestone horizontal hydraulic conductivity has essentially the same effect as an increase in recharge.

Simulations of Alternative Pumping Distributions and the Effects of Drought

Model Representation of Alternative Pumping Distributions

By setting all pumping at wells to zero (evaporative loss from the water bodies is still simulated), the steady-state model can be used to simulate the ground-water system under natural conditions (scenario B). Under these conditions, the greatest change in water level is around the Municipal well and coastal discharge is greater along the east and west shores of the island (fig. 20). Relative to the base-case scenario, the model-calculated position of the freshwater/saltwater interface is a maximum of about 7 ft deeper at the Municipal well when there is no pumping (fig. 21). A 7-ft increase in depth of the freshwater/saltwater interface is about a 17-percent increase in lens thickness relative to the lens thickness calculated using the 1990–97 pumping conditions.

In 2000–01, the pumping distribution is different than the distribution used in the base-case scenario. In 2001, the New Municipal well replaced the old Municipal well and the only other wells in use may be wells TH04 and TH06 (Greg Castro, CUC Deputy Director, oral commun., 2001). Total ground-water withdrawal from wells under these pumping conditions (scenario C) is 972 gal/min (table 4). The model indicates that, relative to the base-case scenario, changing to this pumping distribution has minor effects on the water-level distribution and coastal ground-water discharge (fig. 22) and to the position of the freshwater/saltwater interface (fig. 21). The model-calculated position of the freshwater/saltwater interface beneath the infiltration gallery differs by only about 1 ft relative to the profile from the base-case scenario A.

The maximum pumping distribution shows the effects of pumping all wells that historically have been used for production. This distribution (scenario D) represents the maximum withdrawal probable from the aquifer using existing or currently proposed infrastructure. Total ground-water withdrawal from wells under these pumping conditions is 2,029 gal/min (table 4). With this pumping distribution, model-calculated water levels show a maximum drawdown of about 0.2 ft from the 1990–1997 pumping conditions near the Municipal wells (fig. 23). Ground-water discharge to the coast is reduced most near the middle of both the east and west coasts of the island. The model-calculated position of the freshwater/saltwater interface is about 7 ft shallower beneath the Municipal well area. A 7-ft rise of the freshwater/saltwater interface is about a 17-percent decrease in lens thickness relative to the lens thickness calculated using the 1990–97 pumping conditions.

Effects of Drought

The ground-water flow model developed for this study is currently the best available tool for qualitatively demonstrating the potential hydrologic effects of

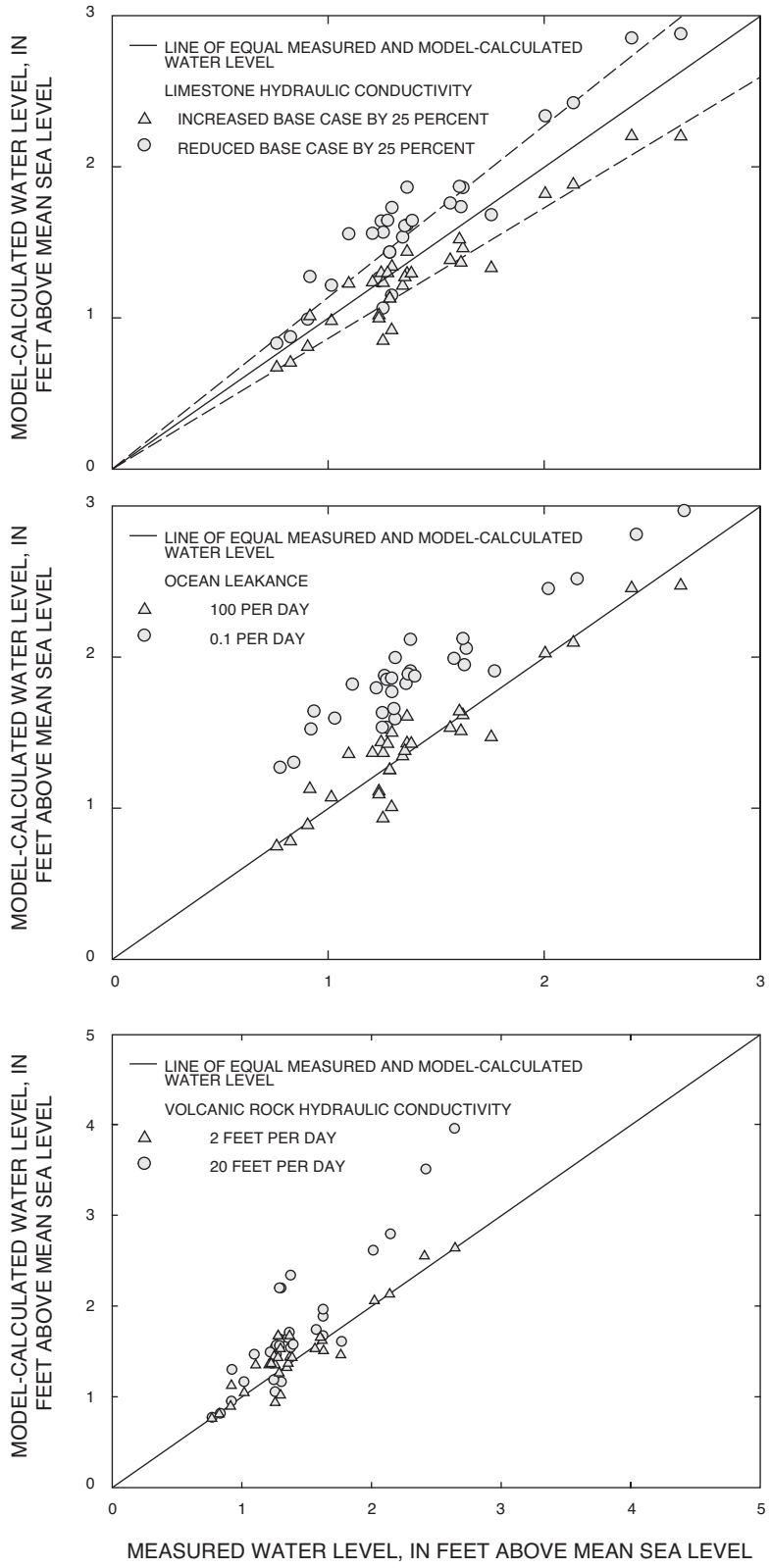

Figure 19. Measured and model-calculated water levels for steady-state pumping conditions, Tinian, for various values of coastal leakance, limestone hydraulic conductivity, and volcanic rock horizontal hydraulic conductivity.

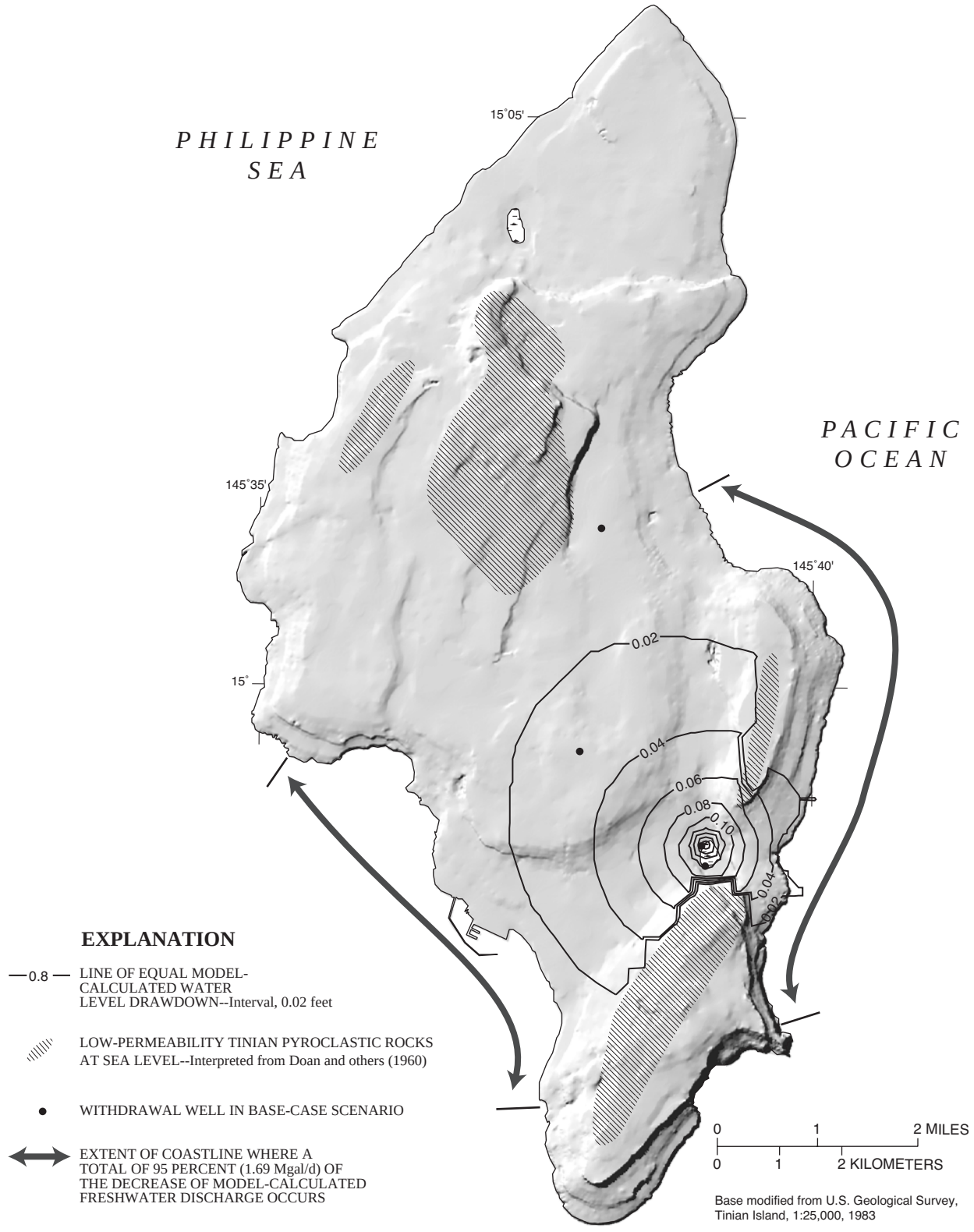

Figure 20. Drawdown in model-calculated water levels and change in coastal discharge from natural conditions (no pumping) to base-case scenario, Tinian.

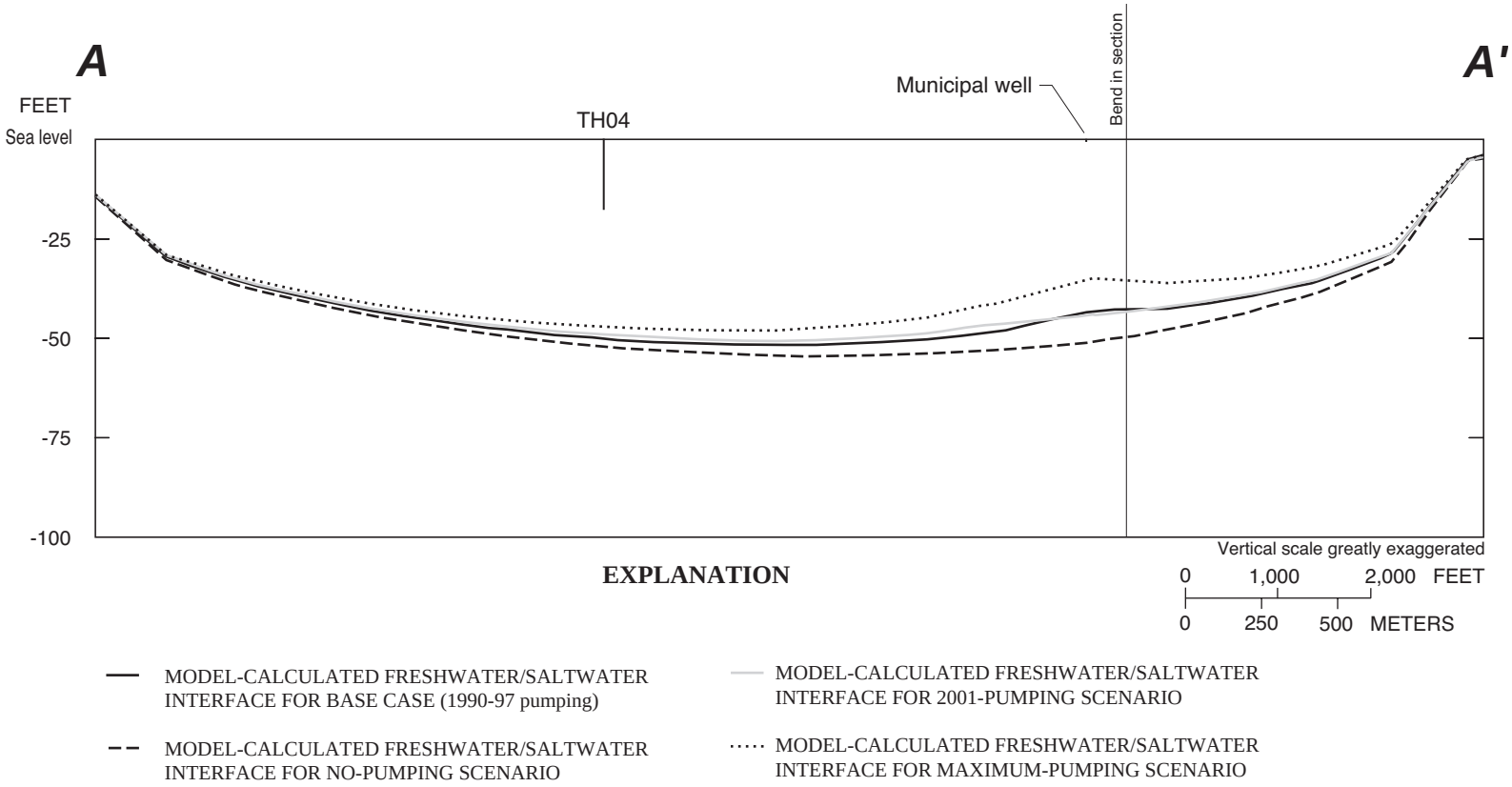

Figure 21. Position of model-calculated interface for base case compared with various scenarios. Line of section is shown in figure 11.

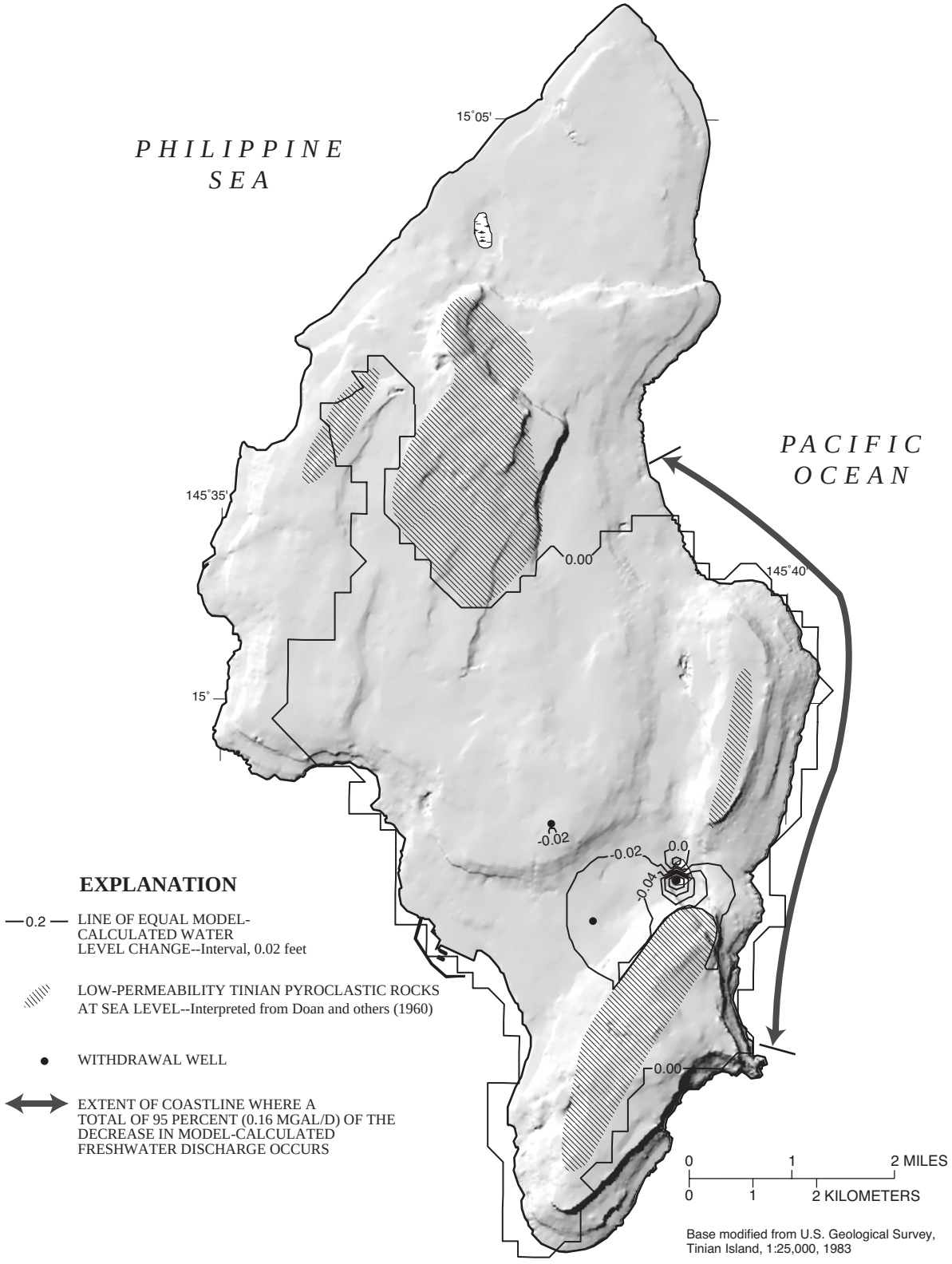

Figure 22. Change in model-calculated water levels and coastal discharge from base-case scenario to 2001-pumping conditions, Tinian.

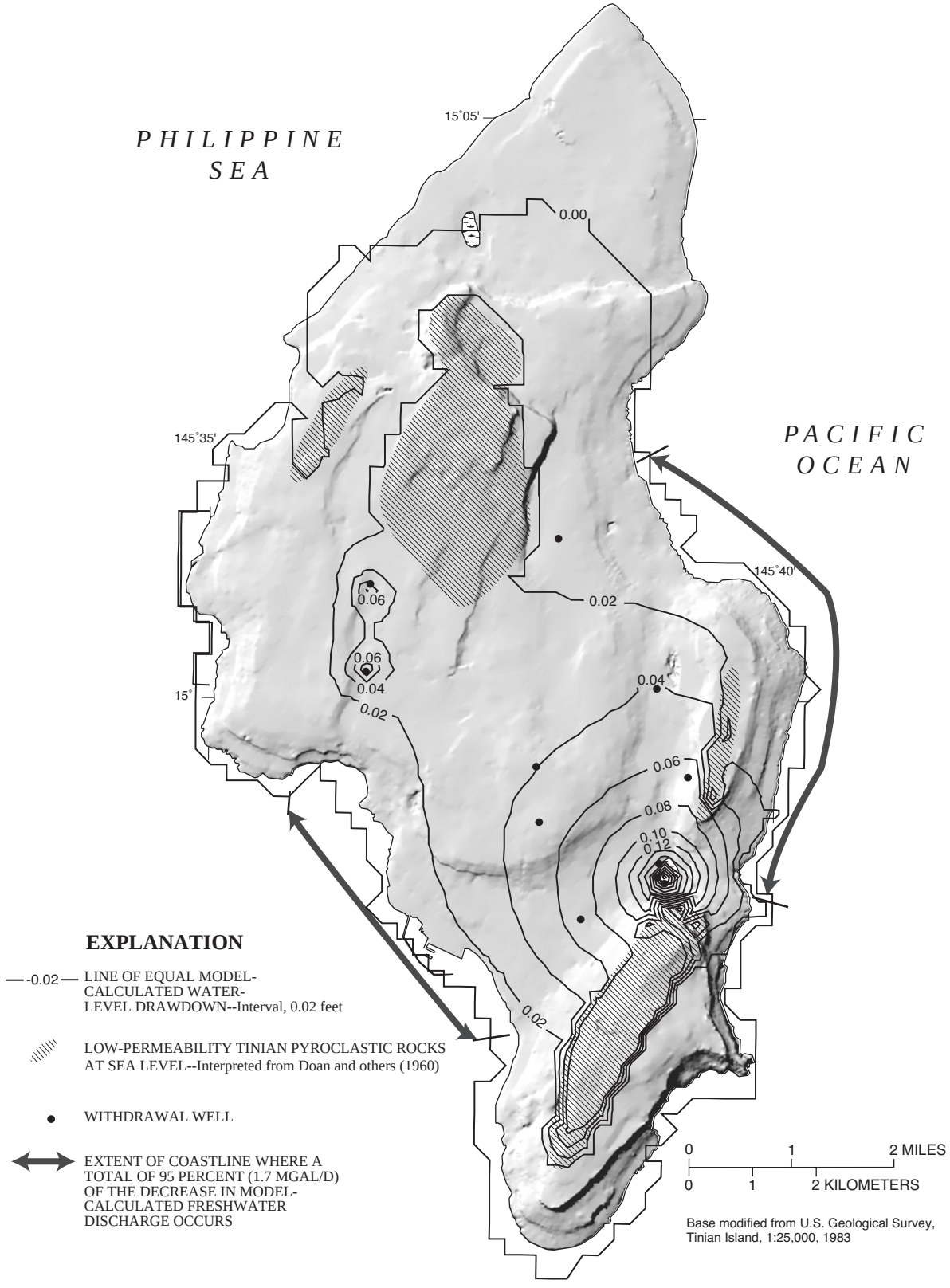

Figure 23. Change in model-calculated water levels and coastal discharge from base-case scenario to maximum-pumping conditions, Tinian.

decreased recharge due to drought on the freshwater-lens thickness. The 1998 drought, which affected Tinian and Saipan, produced a significant decrease in recharge to the freshwater lens. A complete rainfall record from the Tinian airport is not available although data from nearby Saipan can be used to estimate the amount of recharge available from a drought similar in magnitude to the 1998 drought. In 1998, rainfall at Isley Field on Saipan was 35.6 in., 48 percent of the long-term (1954–99) yearly average. The daily water-budget method (described above in the Water Budget section) using the 1998 Isley Field daily rainfall record and the soil-moisture, runoff, and potential evapotranspiration data discussed above for Tinian provided a recharge estimate of 3.1 in. for 1998 on Tinian (about 10 percent of average recharge). Therefore, for Tinian drought simulations, model recharge was reduced to 10 percent of the average conditions and simulations were allowed to proceed for 1 year from the steady-state average conditions. Two pumping scenarios were simulated, 2001 pumping conditions and maximum pumping conditions.

Because the best-fit model is a steady-state model, no attempt was made to match transient model results to observed data. Therefore, best-fit values of aquifer storage properties were not determined through trial-and-error simulation. Aquifer storage properties control the magnitude and rate at which fluid-pressure changes and thus changes in water levels propagate through the aquifer. Higher amounts of aquifer storage cause smaller and slower changes to the freshwater lens and lower amounts cause larger and faster changes. In SHARP, two parameters (porosity and specific storage) are used to define the aquifer storage properties. In the model, porosity is treated as an effective porosity and it affects storage as the water table and the freshwater/saltwater interface move up and down. Karst limestone porosity typically ranges from 5 to 50 percent (Freeze and Cherry, 1979, table 2.4). Specific storage is the parameter in the model that affects the storage associated with the compression or expansion of the aquifer and the water it contains. Specific storage of fractured rock ranges from 1×10^{-6} to 1×10^{-3} ft^{-1} (Streltsova, 1977). Because the value of porosity is three or more orders of magnitude greater than values of specific storage, the effects of varying specific storage in the model are insignificant when compared to the effects of varying porosity, and only the effects of varying porosity were addressed using a series of simulations to bracket the possible range of porosity values for the aquifer. Specific storage was held constant at a value of 1×10^{-5} ft^{-1}.

For 2001 pumping conditions, the rise of the model-calculated freshwater/saltwater interface after 1 year of drought conditions ranged from 3.5 ft to 24 ft for the highest and lowest values, respectively, of porosity (fig. 24). Because the model simulates a sharp interface, it cannot predict the salinity distribution within the aquifer nor is it capable of predicting the quality of water pumped from a given well. To illustrate how the freshwater thickness above the transition zone might vary in different scenarios, the measured thickness of the upper transition zone between the potable limit (250 mg/L chloride concentration) and 50-percent seawater concentration (9,500 mg/L chloride concentration) was determined from figure 12 and superimposed on the position of the freshwater/saltwater interface calculated by the model (fig. 25). Although this technique oversimplifies the effects of pumping on the transition zone, overestimates the true amount of freshwater above the transition zone, and underestimates the potential for saltwater to reach the well, it is still useful to evaluate the potential for saline intrusion into pumped wells.

The simulation with the lowest value of porosity indicates that the freshwater/saltwater interface would have moved high enough to cause both the Municipal well and well TH04 to produce poor-quality water. Operational observations during 1998 indicate that although chloride concentrations did increase, they did not exceed 250 mg/L in any of the wells (Greg Castro, CUC Deputy Director, oral commun., 2001). Therefore, the higher values of porosity (30 to 50 percent) seem more likely to be representative of actual aquifer properties. Operational data show, and the simulations confirm, that the current (2001) pumping distribution likely can be sustained during a year-long drought similar to the drought experienced in 1998.

For maximum pumping conditions, the decrease in the depth of the model-calculated freshwater/saltwater interface ranged from 4 ft to 33 ft for the highest and lowest values, respectively, of porosity (figs. 26 and 27). Simulations using the more-realistic porosity values (30 to 50 percent) indicate the freshwater/saltwater interface would only rise 5 to 8 ft after a 1 year drought similar to the 1998 drought. Therefore, it appears that the freshwater lens could provide adequate freshwater

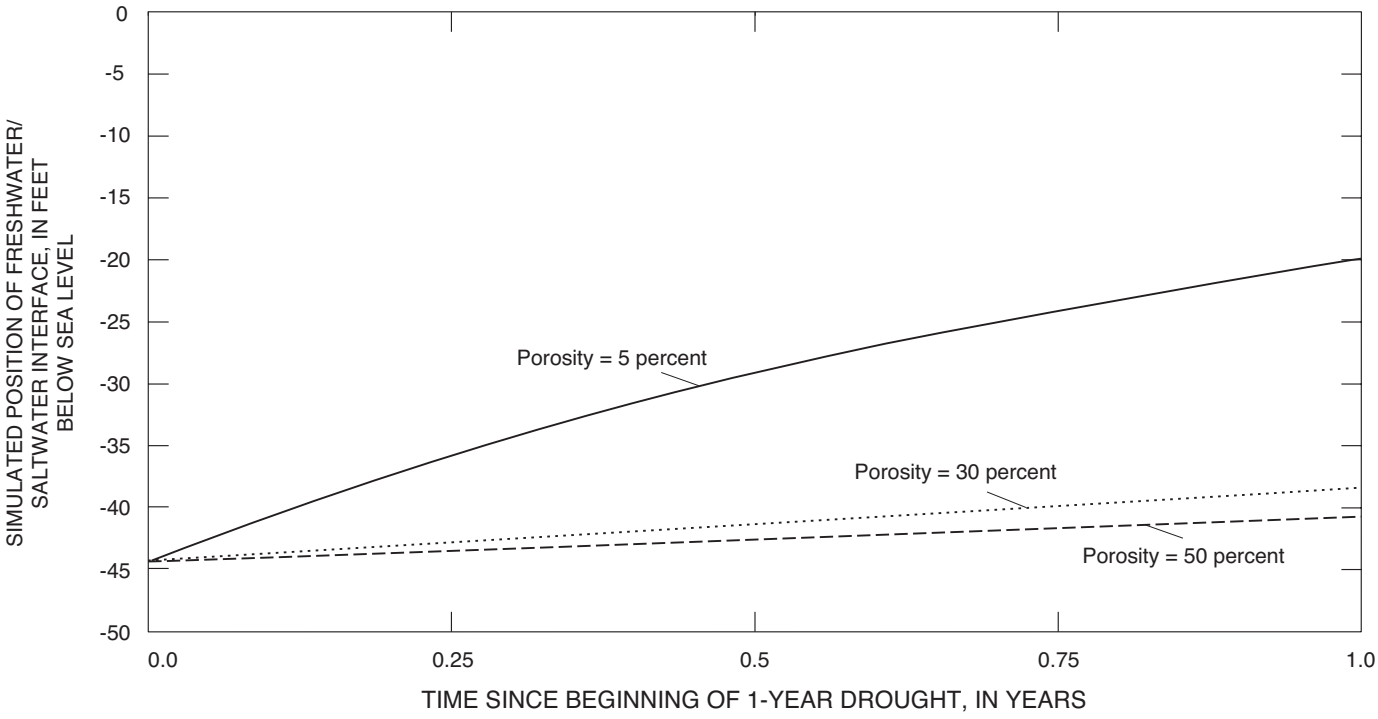

Figure 24. Model-calculated position of freshwater/saltwater interface beneath the municipal well for 2001-pumping conditions during 1-year drought, Tinian.

to the island during a drought similar to the 1998 drought even if pumping were at the maximum conditions based on the existing distribution and depth of wells. However, increasing pumping at any well or adding additional wells too close together will increase the likelihood of saltwater intrusion.

MODEL LIMITATIONS

The steady-state ground-water flow model of Tinian developed for this study has several limitations. Because the model is a sharp interface model, it cannot predict the salinity distribution within the aquifer nor is it capable of predicting the quality of water pumped from a given well. Because of mixing effects, a diffuse transition zone exists near the coast and brackish water exists at the water table in some areas. The model assumes that freshwater and saltwater do not mix. The model simulates the location of the freshwater/saltwater interface but cannot be used to simulate local upconing near pumped wells.

The ground-water flow model cannot accurately predict the local drawdown in or interface rise beneath a pumped well because of the discrete nature of the finite-difference approach and the size of the model cells. Simulated drawdown at a given location in a model cell is represented by the average drawdown for the entire cell. Because the ground-water flow model contains only two relatively thick layers, vertical head gradients can be simulated only to low resolution and model-calculated drawdown may underestimate actual drawdown near partially penetrating wells. However, it also is possible that the model will overestimate drawdown where local geologic conditions are not well represented in the model. The model is, nevertheless, the best currently available tool for predicting the possible hydrologic effects of additional ground-water withdrawals and reduction in recharge due to drought.

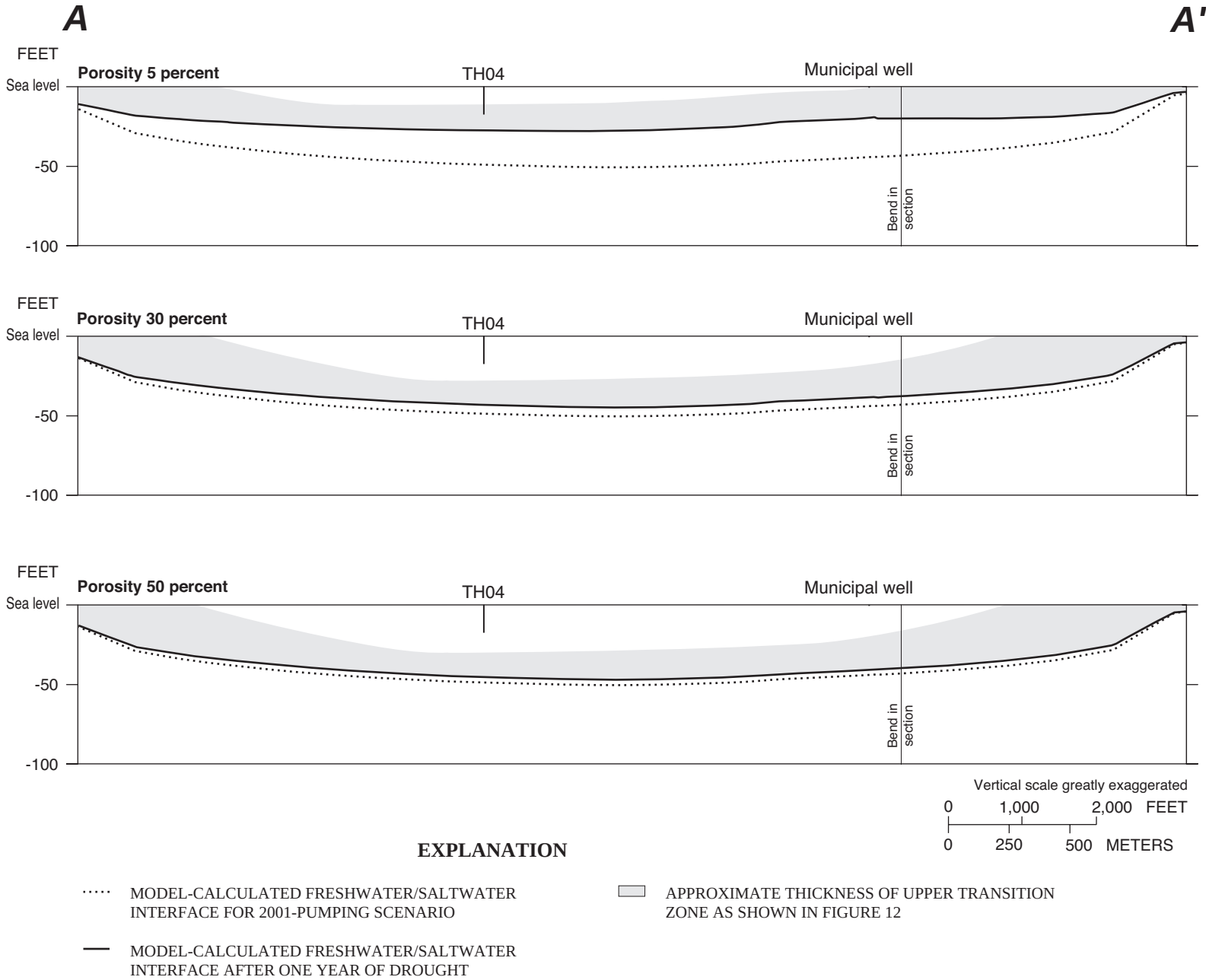

Figure 25. Position of model-calculated interface for 2001 pumping scenario compared with drought scenario for various values of porosity. Line of section is shown in figure 11.

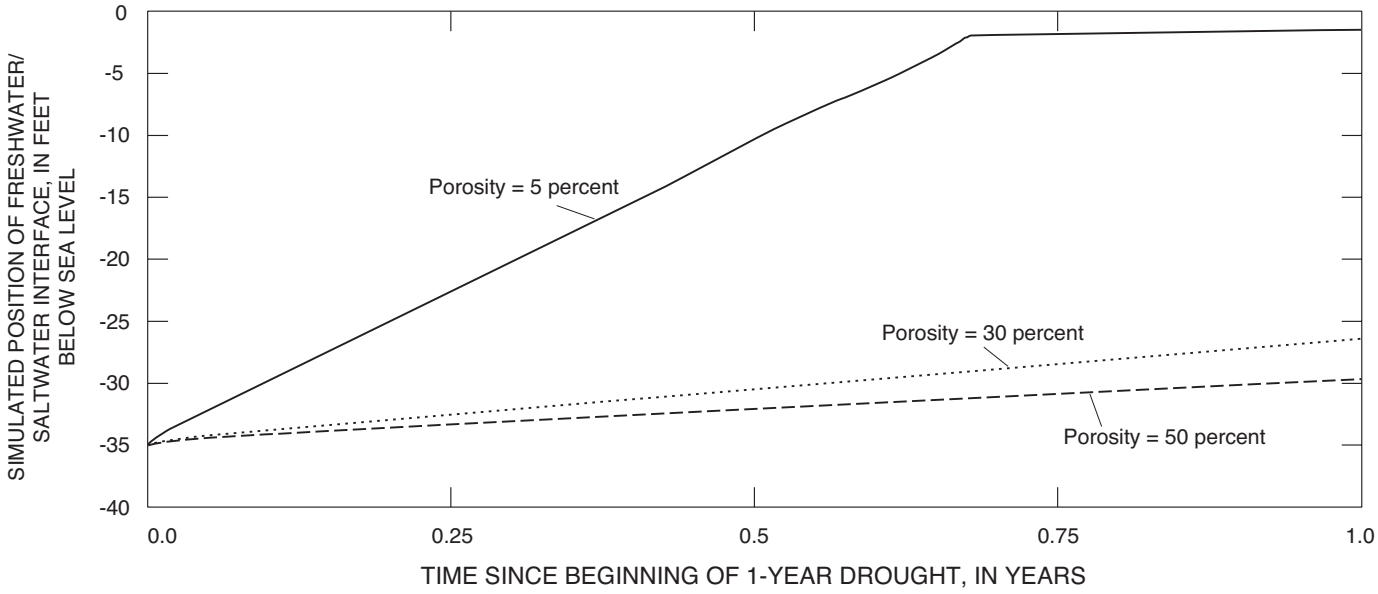

Figure 26. Model-calculated position of freshwater/saltwater interface beneath the municipal well for maximum pumping conditions during 1-year drought, Tinian.

No reliable measurements are available to determine the spatial water-level distribution in the volcanic rocks. Thus, the distributions of model-calculated water levels and freshwater/saltwater interface altitudes are unverified in places.

The model developed for this study is not unique. Different distributions of hydraulic conductivity, coastal leakance, and aquifer thickness could possibly be used in a model to produce equally acceptable model-calculated water levels. Model zones were created to represent areas with less-permeable limestone. Although this zonation fits aquifer-test data, it is probable that other zonations could produce similar acceptable results. The model can be refined and a better representation of the flow system can be obtained as more data become available to constrain the model.

The recharge estimate developed in this study was made using evaporation data from Guam, generalized soil characteristics, and a rough estimate of runoff. There is uncertainty associated with the recharge estimates and the results of the ground-water flow model are limited by this uncertainty.

DATA NEEDS

Additional data can improve the understanding of the ground-water flow system on Tinian. As more data become available, the ground-water flow model can be refined and the accuracy of the model predictions can be improved. Improved recharge estimates can lead to enhanced confidence in ground-water flow model predictions. Monitoring of chloride concentration, ground-water pumpage, and water levels are all necessary to track changes in the freshwater lens, and address whether the changes are related to pumping, recharge, or sea-level changes.

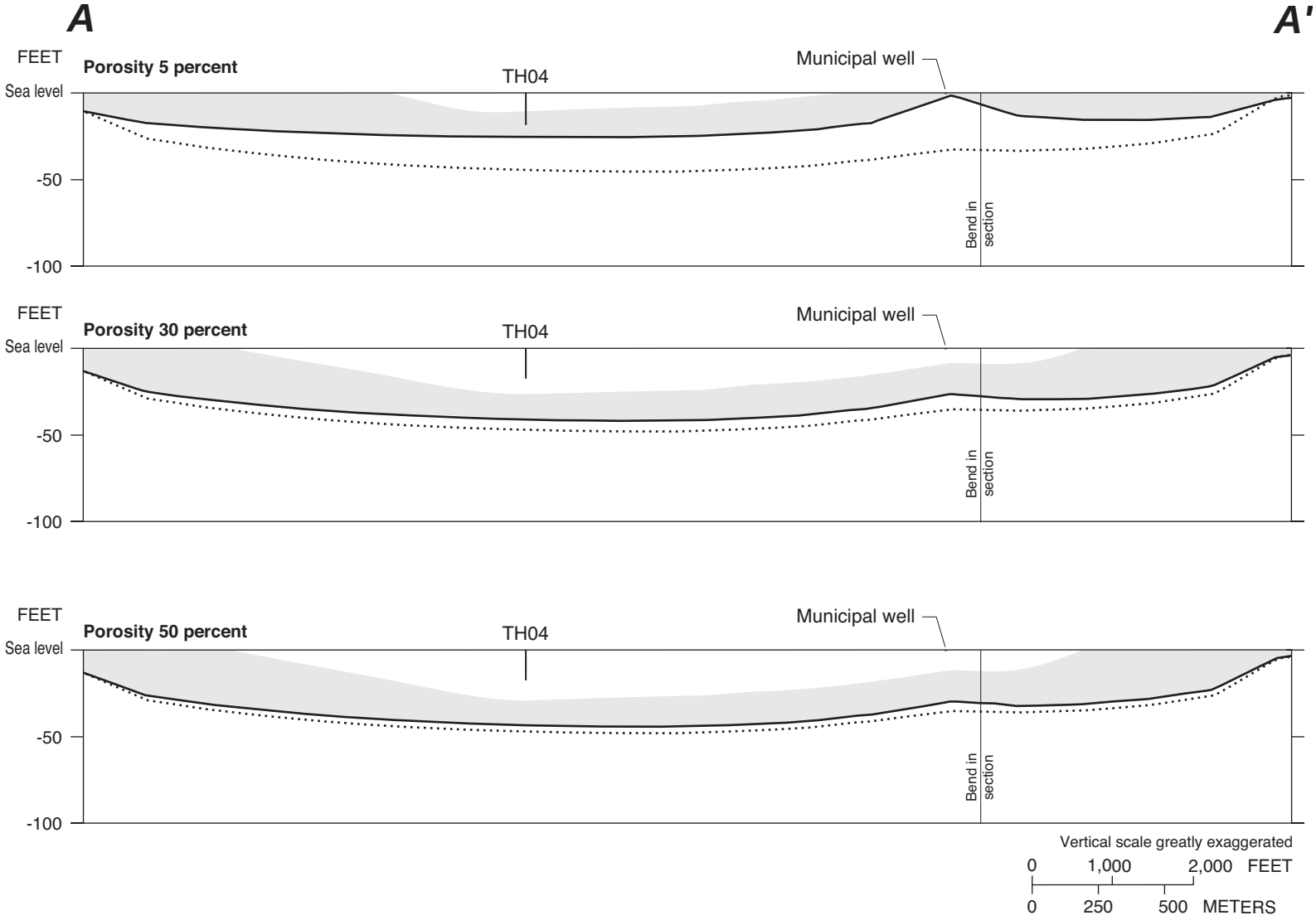

Figure 27. Position of model-calculated interface for maximum pumping scenario compared with drought scenario for various values of porosity. Line of section is shown in figure 11.

SUMMARY AND CONCLUSIONS

The island of Tinian, which is about 12 mi long and as much as 6 mi wide can be divided into five major physiographic areas: the southeastern ridge, the median or Marpo valley, the central plateau, the north-central highland, and the northern lowland. Two wetland areas, Hagoi Lake in the northern lowland and Marpo Marsh in the median valley, are supplied perennially by ground water.

Most public and residential land-use activities take place in a rural setting located in the median valley and parts of the adjacent central plateau and southeastern ridge, occupying about 25 percent of the island. About 75 percent of the island is grassland and secondary forest supporting minor land-use activities.

Four major geologic units make up the island; the Tinian Pyroclastic Rocks, the Tagpochau Limestone, the Mariana Limestone, and unconsolidated sediments consisting of beach deposits, alluvium, and colluvium. The porous nature of coral reefs, and the high susceptibility of limestone to solution weathering favor high hydraulic conductivities in the limestone units. In contrast, hydraulic conductivities of the pyroclastic rocks tend to be low due to poor sorting and the high susceptibility of some volcanic minerals to chemical weathering and alteration to clays. Estimates of limestone hydraulic conductivity from 17 aquifer tests range from 21 to 23,000 ft/d.

Estimates of water-budget components for Tinian are 82 in/yr of rainfall, about 6 in/yr of runoff, 46 in/yr of evapotranspiration, and 30 in/yr of recharge. Rainfall was measured and the other values were estimated using a daily water-budget bookkeeping method.

Ground water is recharged by rainfall infiltration over most of the island. Water-level data indicate that ground water flows generally oceanward radially from the north-central highland and the southeastern ridge. Most of the fresh ground water that is not withdrawn from wells discharges naturally from the aquifer at subaerial and submarine coastal springs. The freshwater-lens system is in limestone and volcanic rocks but the most important ground-water sources are from the freshwater parts of this system in the limestone.

From 1990–97, ground-water withdrawal from the Municipal well averaged about 780 gal/min. Changes in ground-water level on an island can reflect changes in recharge or withdrawal from the ground-water system as well as natural changes in ocean level over hourly to yearly time scales. The most obvious changes in water level occur in response to the ocean tide. Measured daily water-level fluctuations in wells caused by ocean tides are as much as 0.5 ft. In addition to the daily fluctuation in water level caused by the ocean tides, water levels in wells also vary over longer times in response to non-periodic changes in ocean level and to rainfall. Water-level records show variations of as much as 1 ft that correspond closely to the ocean-level record.

Over most of the island, the water table is relatively flat and water levels are less than 2 ft above mean sea level. The highest measured water level in the limestone was 3.42 ft above mean sea level in well M02, which is directly west of the north-central highland. The highest measured water level on the island was in the pyroclastic rocks on the southeastern ridge where the water level was about 90 ft above mean sea level.

Chloride-concentration data indicate that the freshwater lens is thickest in the center of the island near well TH04 and thins toward the east and west coasts. The maximum thickness attained by the freshwater in this section is about 40 ft. The freshwater lens is slightly thinner in the east than in the west, which indicates saltwater may be upconing because of ground-water withdrawal at the Municipal well and evapotranspiration at the Marpo Marsh. The freshwater-lens thickness changes seasonally. The lens thickens after the wet season and thins after the dry season.

A two-dimensional (areal), ground-water flow model using the computer code SHARP (Essaid, 1990) was developed to simulate steady-state ground-water flow on Tinian. The finite-difference grid used in this study covers the entire island of Tinian.

For modeling purposes, Tinian was divided into three horizontal hydraulic-conductivity zones: (1) highly permeable limestone, (2) less-permeable, clay-rich limestone, and (3) low-permeability volcanic rocks. The less-permeable limestone zone was used to simulate the area of higher water levels to the southwest of the north-central highland.

To estimate the hydraulic conductivities of the model zones, average recharge, withdrawals, and water-level conditions were simulated. On the basis of

available information, an average recharge of 29.7 in/yr and average ground-water withdrawal of 854 gal/min was used in the model to simulate 1990–97 conditions. On the basis of modeling results, the following horizontal hydraulic conductivities were estimated: (1) 10,500 ft/d for the highly permeable limestone, (2) 800 ft/d for the less-permeable clay-rich limestone, and (3) 0.2 ft/d for the volcanic rocks. The spatial distribution of model-calculated water levels for this base-case scenario is in good agreement with the set of averaged water-level measurements.

To estimate the hydrologic effects, relative to the base-case scenario, of different pumping distributions on the aquifer, three different steady-state pumping scenarios were simulated. To compare the difference between predevelopment conditions and the base case, a scenario with no ground-water withdrawal was simulated. In the 2001-pumping scenario, the most realistic current distribution (3 wells) and amount (972 gal/min) of ground-water withdrawal was simulated. In the maximum-pumping scenario, all production wells (11 wells) pumping at the designed rate for each well (2,029 gal/min total) was simulated.

The results of the no-pumping scenario showed that the freshwater/saltwater interface beneath the Municipal well would be about 7 ft lower than the base-case scenario and ground-water discharge to the coast would be higher along both the east and west coasts of the center of the island. Model results from the 2001-pumping scenario show little difference from the base-case scenario. The model-calculated altitude of the freshwater/saltwater interface beneath the Municipal well is about 1 ft higher and the reduction of ground-water discharge to the ocean is mainly along the west coast. For the maximum pumping scenario, the model-calculated freshwater/saltwater interface is about 7 ft higher than the position calculated in the base-case scenario.

To estimate the hydrologic effects of drought on the freshwater lens, the 2001- and maximum-pumping scenarios were simulated using three combinations of aquifer porosity covering a range of possible limestone properties. In all scenarios, recharge was reduced to 10 percent of average estimated recharge for one simulated year. The simulations show that the freshwater lens could provide adequate freshwater even under maximum pumping conditions during a drought similar to the one experienced in 1998.

REFERENCES CITED

Baldwin, G.W., 1995, Tinian Magpo watershed and wetland protection plan: prepared for Division of Coastal Resources Management, Department of Lands and Natural Resources, Saipan, 52 p.

Belt, Collins & Associates, 1983, Status and future development of Saipan's water supply.

Brutsaert, Wilfried, 1982, Evaporation into the atmosphere: Boston, Mass., D. Reidel Publishing Company, 299 p.

Bureau of Census, 1996, 1995 census of population and housing, Commonwealth of the Northern Mariana Islands: 248 p.

Cox, D.C., and Evans, J.R., 1956, Section IV – Water Supply *in* Utilities study of sewage and waste disposal, power, roads and water for U.S. Naval Administration Unit, Saipan, Marianas Islands: Belt, Lemmon & Lo, Architects-Engineers Nby 3310, PI-M-4.4L, 109 p.

Doan, D.B., Burke, H.W., May, H.G., and Stensland, C.H., 1960, Military geology of Tinian, Mariana Islands; Chief of Engineers, U.S. Army, variously paginated.

Dunne, Thomas, and Leopold, L.B., 1978, Water in Environmental Planning: New York, W.H. Freeman and Company, 818 p.

Ekern, P.C., 1966, Evapotranspiration of bermudagrass sod, *Cynodon dactylon* L. *Pers*., in Hawaii: Agronomy Journal, v. 58, no. 4, p. 387–390.

Essaid, H.I., 1990, The computer model SHARP, a quasi-three-dimensional finite-difference model to simulate freshwater and saltwater flow in layered coastal aquifer systems: U.S. Geological Survey Water-Resources Investigations Report 90-4130, 181 p.

Freeze, R.A., and Cherry, J.A., 1979, Groundwater: Englewood Cliffs, New Jersey, Prentice-Hall, Inc., 604 p.

Gingerich, S.B., and Yeatts, D.S., 2000, Ground-water resources of Tinian, Commonwealth of the Northern Mariana Islands: Water-Resources Investigations Report 00-4068, 2 sheets.

Harr, M.E., 1962, Groundwater and seepage: New York, McGraw-Hill, 315 p.

Hoffmann, J.P., Carruth, R.L., and Meyer, William, 1998, Geology, ground-water occurrence, and estimated well yields from the Mariana Limestone, Kagman Area, Saipan, Commonwealth of the Northern Mariana Islands: U.S. Geological Survey Water-Resources Investigations Report 98-4077, 38 p.

Izuka, S.K., and Gingerich, S.B., 1998, Ground water in the Southern Lihue Basin, Kauai, Hawaii: U.S. Geological Survey Water-Resources Investigations Report 98-4031, 71 p.

Lawlor, J.P., 1946, Skimming trench solves a coral island water supply problem: Engineering News-Record, v. 137, p. 993–995.

Linsley, R.K., Jr., Kohler, M.A., and Paulhus, J.L., 1982, Hydrology for Engineers (3d ed.): New York, McGraw-Hill, 508 p.

National Climatic Data Center, 2000, Digital precipitation and evaporation data for Pacific islands, downloaded from <http://ols.nndc.noaa.gov/olstore.html> on December 20, 1999.

Nullet, Dennis, 1987, Water balance of Pacific atolls: Water Resources Bulletin, American Water Resources Association, v. 23, no. 6, p. 1,125–1,132.

Polubarinova-Kochina, P.Ya., 1962, Theory of ground water movement: Princeton, Princeton University Press, 613 p.

Streltsova, T.D., 1977, Storage properties of fractured formations, *in* Dilamarter, R.R. and Csallany, S.C. eds., Hydrologic Problems in Karst Regions: Bowling Green, Kentucky, Western Kentucky University, p. 188–192.

Thornthwaite, C.W., and Mather, J.R., 1955, The water balance: Publications in Climatology, v. 8, no. 1, p. 1–104.

Todd, D.K, 1980, Groundwater Hydrology: New York, Wiley, 535 p.

Underwood, M.R., Peterson, F.L., and Voss, C.I., 1992, Groundwater lens dynamics of atoll islands: Water Resources Research v. 28, no. 11, p. 2,889–2,902.

U.S. Department of Agriculture, 1994, Island resource study, Tinian, Commonwealth of the Northern Mariana Islands, 50 p.

Veihmeyer, F.J., and Hendrickson, A.H., 1955, Does transpiration decrease as the soil moisture decreases?: Transactions, American Geophysical Union, v. 36, no. 3, p. 425–448.

Weast, R.C., Lide, D.R., Astle, M.J., and Beyer, W.H., eds., 1989, CRC handbook of chemistry and physics (70th ed.): Boca Raton, Fla., CRC Press, variously paged.

Young, F.J., 1989, Soil survey of the islands of Aguijan, Rota, Saipan, and Tinian, Commonwealth of the Northern Mariana Islands: U.S. Department of Agriculture, Soil Conservation Service, 166 p.